

Electron-Transfer Reactions at Silicon/Liquid Interfaces

Arnel M. Fajardo and Nathan S. Lewis, Division of Chemistry and Chemical Engineering, California Institute of Technology

Abstract

This article describes theoretical models for, and experimental data on, the rates of interfacial electron-transfer processes at semiconductor/liquid contacts. These systems are of practical interest because such electron transfers are a critical factor in understanding the behavior of photoelectrochemical cells as energy conversion devices. The general principles of these processes, a discussion of past and present experimental data, and a comparison between theoretical expectation and experimental observations on a variety of semiconductor electrode systems, are the main focus of this article.

Semiconductor/liquid junctions provide the most efficient wet chemical method presently known for converting sunlight into chemical or electrical energy.^{1,2} In such systems, sunlight is absorbed by a semiconducting photoelectrode, and the electron-hole pair produced by the light absorption is converted into a photocurrent (Figure 1). Quantum yields for photocurrent production can approach unity for wavelengths of light spanning the near infrared and visible regions of the spectrum, and the overall solar optical-to-energy conversion efficiencies of such devices can be in excess of 15%.¹

The basic processes of light absorption and charge separation at semiconductor/liquid contacts are well-understood.¹⁻³ Absorption of photons above the band gap energy of the semiconductor leads to creation of electron-hole pairs in the solid. A strong electric field, present at the solid/liquid interface, then separates the electron and the hole, typically in < 1 ps. At an n-type semiconductor/liquid contact (shown in Figure 1), the electric field drives the minority carriers, i.e., the holes, toward the solid/liquid contact and drives the majority carriers, i.e., the electrons, into the bulk of the semiconductor.

Continued on page 3

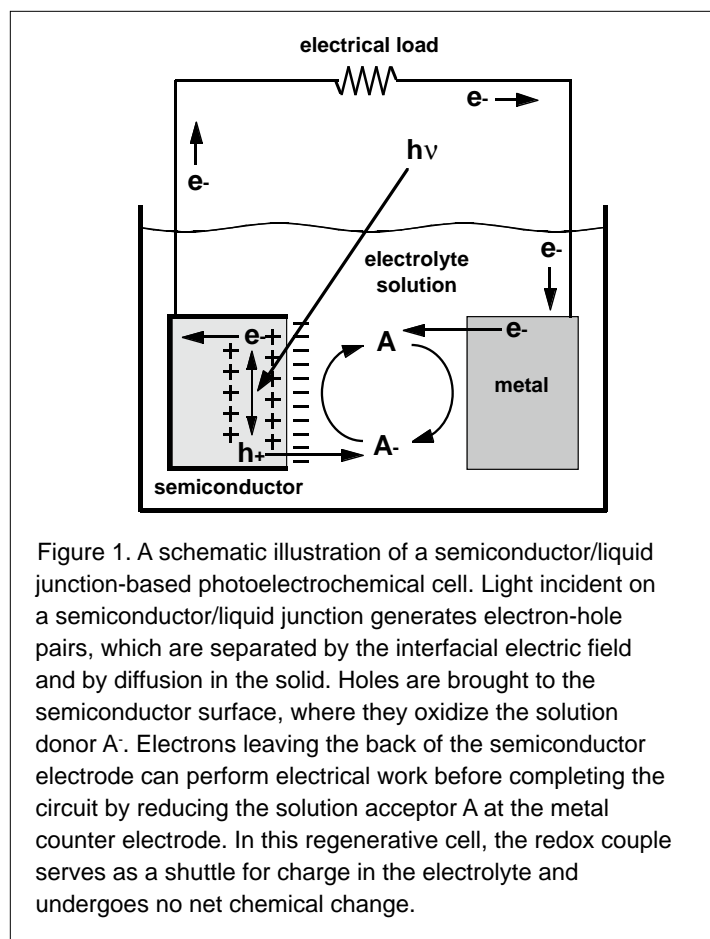


Figure 1. A schematic illustration of a semiconductor/liquid junction-based photoelectrochemical cell. Light incident on a semiconductor/liquid junction generates electron-hole pairs, which are separated by the interfacial electric field and by diffusion in the solid. Holes are brought to the semiconductor surface, where they oxidize the solution donor A. Electrons leaving the back of the semiconductor electrode can perform electrical work before completing the circuit by reducing the solution acceptor A at the metal counter electrode. In this regenerative cell, the redox couple serves as a shuttle for charge in the electrolyte and undergoes no net chemical change.

From the Executive Director

D.C. Neckers, Executive Director, Center for Photochemical Sciences, Bowling Green State University

I recently received the 1996 Annual Report from the Research Corporation. Founded in 1912, the Research Corporation was the fulfillment of the philanthropic dream of Frederick Gardner Cottrell, assisted by Charles Doolittle Wolcott, Secretary of the Smithsonian Institution. The purpose was to make inventions and patent rights more available and effective in arts and manufacture and to provide the means for research and experimentation at scholarly institutions. Cottrell's brilliant idea about philanthropy has seeded the research of many, many Nobel laureates.

My contact with the Research Corporation began in the early 1960s. After I accepted my first teaching position, I wrote a Research Corporation office in Chicago indicating I was moving to a teaching position in the fall of the year, and the Research Corporation would be extremely lucky to support my research program (here was my Nobel prize winning idea) at (astronomical number) a year. Please send the check to ... (probably me).

Soon I received a letter from a secretary indicating the RC program director for my region was no longer there and someone would be in touch. A letter subsequently arrived informing me my proposal was completely out of line with current funding guidelines. An application form for applying for a more modest RC grant was included. I dutifully filled out the form enclosed, returned it and waited for my check. Somewhat later I received a second letter saying that my proposal wasn't worth funding. The letter said that one of the reviewers had said "Neckers must not have thought about this experiment much ... the deuterium proposition makes no sense."

After harrumphing around the room for a day or two, someone convinced me to reread my proposal. When I did so, I discovered that my prize-winning idea had been obfuscated in terribly unclear English. A rewrite carefully edited by another provided the reviewer a better idea of what I wanted to do and in six months or so I received a \$2,000 research grant.

The Research Corporation Annual Report carries the autobiographical account of the career of Brian Andreen, grants administrator and Vice President, who is retiring this year. Brian was one of a small group of grants administrators at the Research Corporation who sought out good science in small places and who had the unenviable responsibility of sending letters to brash youngsters, like I was then, declining their research proposal. When I first knew Brian, he would arrive in my office at Hope College unannounced and usually at a strange hour. We'd talk for a few minutes and then he would go to another's office. I enjoyed talking with him and telling him about my work. But the very fact that I was in my labs at an unusual hour was what Brian was really looking for. In 15 minutes he had discovered more about me and my research program than he would ever learn from pages upon pages of proposal.

I've known and respected Brian Andreen since 1964. I even served a term on the Research Corporation Program Advisory Committee. In fact, at some time in the deep dark past I identified Mike Doyle from among a cadre of applicants as the person we wanted to replace Jerry Mohrig on the faculty at Hope College. Hope was Mike's first job. Mike was announced last summer as Brian's immediate replacement.

Brian began, in science, when grants administrators had to seek out scientists who could, or would, do research in colleges. Our young scientific colleagues likely can't believe there was such a day, but there was. On behalf of all academic scientists, Brian, we thank you and so many of your colleagues for being our advocate and for helping us shape our programs and careers. Your behind-the-scenes contributions, particularly to science and scientists teaching in smaller colleges and universities, were extremely important in the formative times after Sputnik.

In This Issue

Electron-Transfer Reactions at Silicon/Liquid Interfaces	1
Collisional Deactivation of Large, Highly Vibrationally Excited Molecules	7
Time Resolved ESR and CIDNP Spectroscopy: Two Versatile Tools for the Investigation of Photoinitiators	13

Continued from page 1

The energy storage process is completed if these holes undergo interfacial charge transfer to the donors in the electrolyte prior to the occurrence of any recombination events. Similar processes occur at a p-type semiconductor/liquid contact, except that the sign of the electric field is reversed. Chemical control over these processes, achieved through formation of a nearly electrically perfect junction, optimization of the electric field strength at the semiconductor/liquid interface, and minimization of recombination processes in the bulk and at the surface of the semiconductor electrode, have led to a number of stable, efficient, and promising photoelectrochemical energy conversion devices.¹

Obviously, regardless of the type of semiconductor doping that is used, understanding the interfacial charge-transfer events is critical to understanding the operation of the entire photoelectrochemical cell. The interfacial kinetic processes control both the "forward" minority carrier reaction that leads to photocurrent as well as the undesirable "back" electron transfer (majority carriers crossing the interface) that instead merely results in recombination. For a semiconductor electrode, the rate law for interfacial charge transfer from a delocalized charge carrier in the solid to a nonadsorbing, randomly dissolved, electron acceptor in the solution phase is as follows:⁴

$$J = -q k_{\text{et}} n_s [A] \quad (1)$$

where q is the charge on an electron, n_s is the electron concentration at the surface of the solid, and $[A]$ is the concentration of the electron acceptor in the interphase region of the solid/liquid contact. With n_s and $[A]$ measured in units of cm^{-3} , and J representing a current density, k_{et} has units of $\text{cm}^4 \text{s}^{-1}$. This second-order rate law is obtained because unlike the situation at a metal electrode, at a semiconductor, n_s is a variable that can be measured and that can be controlled experimentally (by changing the electrode potential). This surface electron concentration must thus be explicitly represented in the rate expressions.

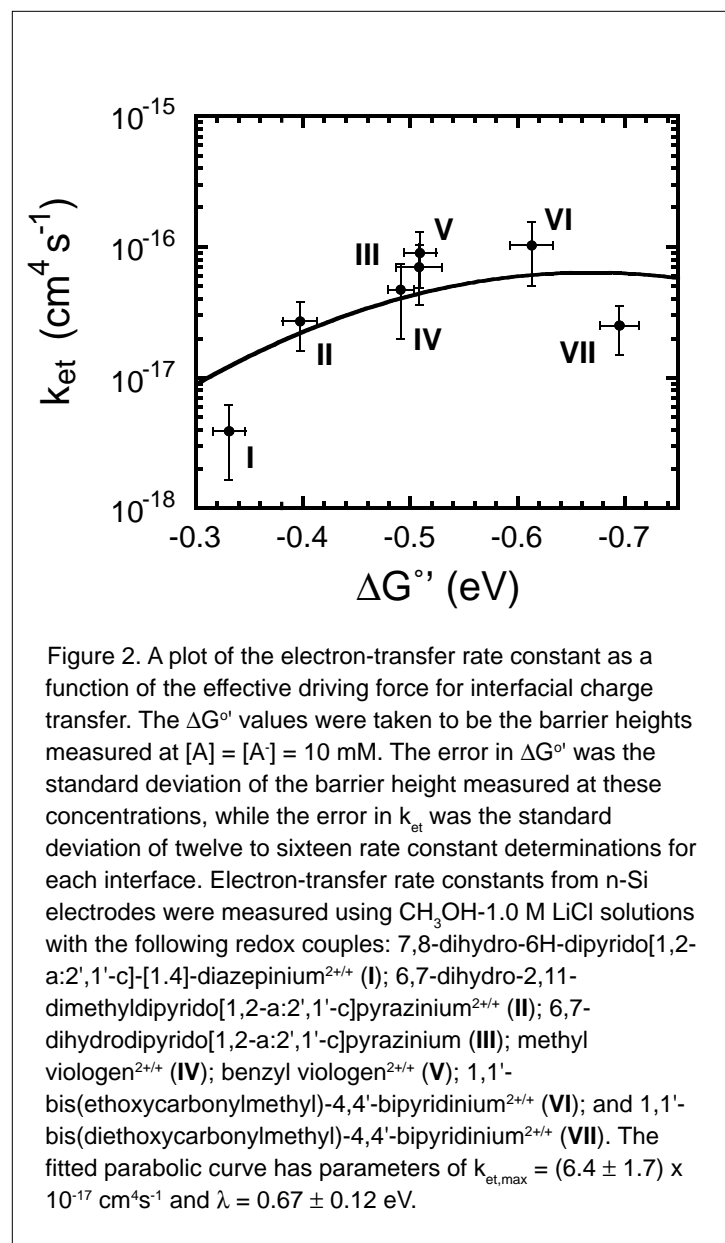
Measurement of the rate constant, k_{et} , clearly requires measurement of both n_s and J , as well as validation of the second-order rate law of eq 1. Measurements of k_{et} , however, despite being simple in principle, have been elusive for over four decades. Such measurements have been thwarted by the poorly understood, nonideal behavior of many semiconductor/liquid contacts,^{5,6} by the instability of most semiconductor electrodes in aqueous electrolytes,² and by the inability to perform a systematic study of the interfacial kinetic processes for a homologous series of one-electron, outer-sphere redox systems having similar reorganization energies.

In the late 1960s, Morrison and co-workers used steady-state current density-potential methods to attempt to determine rate constants for several species at n-type ZnO electrodes.⁷ In many of these cases, the n-ZnO/liquid contacts exhibited the expected first order dependence on n_s , but only some systems displayed the first order dependence on the concentration of acceptor, $[A]$. Measurements of heterogeneous electron-transfer rates at the n-ZnO/ H_2O - $\text{Fe}(\text{CN})_6^{3-/4-}$ junction yielded a k_{et} of $10^{-18} \text{ cm}^4 \text{ s}^{-1}$. This value agrees qualitatively with theory, but it is not clear that $\text{Fe}(\text{CN})_6^{3-/4-}$ is a nonadsorbing redox couple. Attempts to fit the data for n-ZnO obtained with several redox couples to a free energy vs k_{et} dependence were thwarted by the obvious lack of a constant reorganization energy for the various, simple metal-ion-based, redox systems that were available at the time. In addition, many of these ions are well-known to adsorb onto oxide/hydroxide surfaces, and there is a significant possibility of inner-sphere electron-transfer processes between the ion and the electrode for many of the systems studied. Finally, some systems, such as $\text{Fe}(\text{CN})_6^{3-/4-}$, displayed rate constants that changed as the pH of the solution was varied, even though the changes in driving force due to the change in pH were estimated to be sufficiently small that little change in k_{et} should have been observed.⁸ Little follow-up of these measurements was performed during the ensuing three decades.

Recent work from our laboratory has shown that these drawbacks can be largely overcome through use of n-type Si electrodes in CH_3OH with a series of viologens as the soluble one-electron acceptors.⁹ Si electrodes are stable towards passivation or corrosion reactions in dry methanol,¹⁰ and the driving force for interfacial charge transfer can be varied in this solvent system through the use of a homologous series of viologen^{2+/+} redox species. Furthermore, such interfaces appear to exhibit simple and nearly ideal energetic and kinetic behavior.⁹ The ability to vary the energetics for the interfacial charge-transfer event makes it possible to investigate the predictions of Marcus theory with regard to the variation in rate constant as function of driving force at the semiconductor/liquid contact.⁴ In addition, such measurements allow experimental determination of the maximum charge-transfer rate constant at optimal exoergicity for such contacts, thereby allowing an estimate of the electronic coupling between the delocalized charge carriers in the semiconductor electrode and the localized electron acceptors in the solution phase.

These studies have recently been reported in the literature.⁹ The n-Si/ CH_3OH -viologen^{2+/+} system does indeed seem to exhibit ideal energetic and kinetic behavior, allowing for a direct, steady-state measurement of k_{et} for various

viologens. Figure 2 displays the compilation of these measurements, in the form of a plot of k_{et} vs the effective driving force for interfacial charge transfer, ΔG° , for each of the n-Si/CH₃OH-viologen^{2+/+} contacts studied to date. Several conclusions are obvious from this plot. First, the maximum rate constant values are clearly in the range of $k_{\text{et,max}} = 10^{-17}$ - 10^{-16} cm⁴ s⁻¹. Second, the rate constants are reasonably well-fit by the expected dependence of k_{et} on ΔG° as given by the classical Marcus expression for electron-transfer processes.



These rate constant measurements are in excellent accord with theoretical expectations. In the simplest approximation, the value of the maximum charge-transfer rate constant at a metal/liquid interface predicted by Marcus both classically and quantum-mechanically, 10^5 cm⁵ s⁻¹,¹¹ can be divided by the electron concentration at the surface of the metal, because the electron concentration in the electrode is implicit in the rate constant expression for a metal electrode but the surface electron concentration is explicitly present in the rate law expression of eq 1 for a semiconductor electrode. The electron concentration at the Fermi level of various metals is typically 10^{22} cm⁻³,¹² so the collision-based model yields $k_{\text{et,max}} \approx (10^5 \text{ cm}^5 \text{ s}^{-1}) / (10^{22} \text{ cm}^{-3}) \approx 10^{-17}$ cm⁴ s⁻¹.

More sophisticated models that have been applied to this system include semiclassical collision treatments, adaption of Marcus' treatment for liquid/liquid contacts to semiconductor/liquid contacts, and a quantum-mechanically based Fermi Golden Rule approach to relating the coupling in homogeneous donor/acceptor electron-transfer events and events at metal electrodes to the charge-transfer kinetics at semiconductor electrodes.^{4,13} All of these treatments are remarkably consistent, and yield values for $k_{\text{et,max}}$ i.e. the rate constant at optimal exoergicity, of 10^{-17} - 10^{-16} cm⁴ s⁻¹. The experimental values for transfer of delocalized charge carriers from a semiconductor to the viologen^{2+/+} systems are therefore in excellent agreement with theoretical expectations based on our body of knowledge accumulated to date in other molecule-based electron-transfer processes.

These rate constant measurements also provide insight into numerous aspects of the behavior of photoelectrochemical cells as energy conversion devices. It is well-documented that the photovoltages produced by illuminated semiconductor/liquid contacts

can be much higher than those obtained from semiconductor/metal contacts using the same types of semiconducting substrates.¹ This can be readily understood, because with a $k_{\text{et,max}} = 10^{-16}$ cm⁴ s⁻¹ and a concentration of redox species of $0.1 \text{ M} = 6 \times 10^{19}$ cm⁻³, the effective interfacial carrier collection velocity is only $(10^{-16} \text{ cm}^4 \text{ s}^{-1})(6 \times 10^{19} \text{ cm}^{-3}) = 6 \times 10^3$ cm s⁻¹. In contrast, the collection velocity at a semiconductor/metal contact is typically 10^7 cm s⁻¹, because the metal has a continuum of states available to collect essentially every electron that arrives at the solid/liquid contact and because these electrons arrive at a thermal velocity of 10^7 cm s⁻¹ to the interface. Thus, even identical barrier heights would produce less interfacial majority carrier current, and therefore less recombination, at a semiconductor/liquid contact than at a semiconductor/metal contact. This produces higher open-circuit voltages, and higher energy conversion efficiencies, for the semiconductor/liquid contacts relative to semiconductor/metal systems, as is observed experimentally.

This value of $k_{\text{et,max}} = 10^{-17}$ - 10^{-16} $\text{cm}^4 \text{s}^{-1}$ is also consistent with the slow time decays of the Si/CH₃OH-1,1'-dimethylferrocene^{+ / 0} contact that have been observed in microwave conductivity experiments.¹⁴ It is also consistent with the differences in spectral response data at semiconductor/liquid and semiconductor/metal contacts and explains the absence of observable recombination at short wavelength for the semiconductor/liquid contacts.¹⁵ Additionally, it explains why no outer-sphere redox systems have been able to effectively stabilize small-band-gap semiconductors in contact with aqueous electrolytes: compared to the 55 M concentration of water that can participate in anodic oxidation or corrosion processes, it is not possible to scavenge effectively all of the photogenerated minority carriers with a $k_{\text{et,max}}$ of 10^{-16} $\text{cm}^4 \text{s}^{-1}$, even at hole acceptor concentrations of > 1 M. Hence, electrode stability is only observed for high concentrations of adsorbing redox species such as Se²⁻ or Te²⁻ on GaAs, S²⁻ on CdS, I⁻ on n-GaAs, and similar systems. In aqueous solution, outer-sphere redox couples would thus only be expected to be effective in competing with very slow photocorrosion processes, but these systems could, of course, be exploited to produce a variety of stable photoelectrochemical cells in dry nonaqueous solvents. Again these predictions are in excellent accord with experimental observations.

Finally, these rate constant values are in excellent agreement with most other experimental results on semiconductor electrodes. Scanning electrochemical microscopy techniques have been used to measure a k_{et} of 5.7×10^{-17} $\text{cm}^4 \text{s}^{-1}$ at the p-WSe₂/H₂O-Ru(NH₃)₆^{3+ / 2+} interface.¹⁶ Substituting reasonable estimates of the driving force for charge transfer of = -1.09 eV and the reorganization energy of 1.5 eV into the conventional Marcus nuclear reorganization term results in a $k_{\text{et,max}}$ at optimal exoergicity of 2×10^{-16} $\text{cm}^4 \text{s}^{-1}$. A recent study of the n-InP/CH₃OH junction estimated that $k_{\text{et,max}} = 10^{-16}$ $\text{cm}^4 \text{s}^{-1}$ for redox couples such as dimethylferrocene^{+ / 0} and 1,1'-diphenyl-4,4'-bipyridinium^{2+ / +}.¹⁷ Differential capacitance measurements have yielded a k_{et} of 10^{-18} $\text{cm}^4 \text{s}^{-1}$ for the p-GaAs/HCl(aq)-Cu^{2+ / +} interface,¹⁸ which when corrected for the nuclear terms, also resulted in an estimate of $k_{\text{et,max}} = 10^{-16}$ $\text{cm}^4 \text{s}^{-1}$. It is not clear that this interface consists of an outer-sphere, nonadsorbing redox system, so the agreement in this case between theory and experiment might be fortuitous. A few measurements of extremely high k_{et} values, between 10^{-12} and 10^{-10} $\text{cm}^4 \text{s}^{-1}$, have been claimed in recent years,¹⁹ but these systems have been found in subsequent, more complete work to be plagued by adsorption and/or by other complications which cast serious doubt on the use of these interfaces to allow determination of second-order rate constants within the framework of transfer of delocalized charge carriers in the solid to randomly distributed, nonadsorbing, outer-sphere redox species in the solution phase.²⁰

Although much progress has been clearly made in this area in recent years, this field still seems to hold promise for future important developments. Experiments such as those being performed by D. Waldeck and co-workers,²¹ focused on elucidating the distance dependence of electron transfer at semiconductor/liquid contacts, are obviously significant and important. Conclusive experimental observation of the Marcus inverted region for outer-sphere redox reagents has not yet been reported, to our knowledge, nor have data been reported that demonstrate unambiguously the predicted effects of changing the reorganization energy of the ion on the measured interfacial charge-transfer rate constant. Some of the reorganization energy in these interfacial electron-transfer events might well be due to solvation of electrons near the surface of the electrode, and also possibly to some nuclear reorganization of the bonds in the near-surface region of the solid itself. No clear-cut experimental evidence is available to address these points at the present time. Refinements in the theoretical description of such processes, including more accurate descriptions of the band structure of the electrode, of the distance dependence of the reorganization energy of the acceptor, and of the possible role of quantum vibrational modes in such systems, also await a thorough description. One of our goals in preparation of this article was to acquaint the reader with the advances that have been made in this area in recent years, while another goal is to stimulate further interest in these problems within the photochemical community.

Acknowledgment

The work summarized in this article was supported by the National Science Foundation and by the Department of Energy, Office of Basic Energy Sciences.

References

1. Tan, M.X.; Laibinis, P.E.; Nguyen, S.T.; Kesselman, J.M.; Stanton, C.E.; Lewis, N.S. *Prog. Inorg. Chem.* **1994**, *41*, 21.
2. Wrighton, M.S. *Acc. Chem. Res.* **1979**, *12*, 303.
3. Gerischer, H. In *Solar Energy Conversion. Solid-State Physics Aspects*; Seraphin, B.O., Ed.; Springer-Verlag: Berlin, 1979; Vol. 31; pp 115.

4. Lewis, N.S. *Annu. Rev. Phys. Chem.* **1991**, *42*, 543.
5. Howard, J.N.; Koval, C.A. *Anal. Chem.* **1994**, *66*, 4525.
6. Bard, A.J.; Bocarsly, A.B.; Fan, F.-R.F.; Walton, E.G.; Wrighton, M.S. *J. Am. Chem. Soc.* **1980**, *102*, 3671.
7. Morrison, S.R. *Surf. Sci.* **1969**, *15*, 363.
8. Freund, T.; Morrison, S.R. *Surf. Sci.* **1968**, *9*, 119.
9. (a) Fajardo, A.M.; Lewis, N.S. *Science* **1996**, *274*, 969. (b) Fajardo, A.M.; Lewis, N.S. *J. Phys. Chem. B*, in press.
10. Shreve, G.A.; Karp, C.D.; Pomykal, K.E.; Lewis, N.S. *J. Phys. Chem.* **1995**, *99*, 5575.
11. Marcus, R.A. *J. Phys. Chem.* **1991**, *95*, 2010.
12. Kittel, C. *Introduction to Solid State Physics*; 6th ed.; Wiley: New York, 1986.
13. Royea, W.J.; Fajardo, A.M.; Lewis, N.S. *J. Phys. Chem. B*, in press.
14. Forbes, M.D.E.; Lewis, N.S. *J. Am. Chem. Soc.* **1990**, *112*, 3682.
15. Kumar, A.; Lewis, N.S. *J. Phys. Chem.* **1990**, *94*, 6002.
16. Horrocks, B.R.; Mirkin, M.V.; Bard, A.J. *J. Phys. Chem.* **1994**, *98*, 9106.
17. Pomykal, K.E.; Lewis, N.S. *J. Phys. Chem. B* **1997**, *101*, 2476.
18. Uhlendorf, I.; Reineke-Koch, R.; Memming, R. *J. Phys. Chem.* **1996**, *100*, 4930.
19. Rosenwaks, Y.; Thacker, B.R.; Nozik, A.J.; Ellingson, R.J.; Burr, K.C.; Tang, C.L. *J. Phys. Chem.* **1994**, *98*, 2739.
20. (a) Nozik, A.J. Presented at the 211th National Meeting of the American Chemical Society, New Orleans, LA, March 1996; Paper PHYS 11. (b) Pomykal, K.E.; Fajardo, A.M.; Lewis, N.S. *J. Phys. Chem.* **1996**, *100*, 3652. (c) Bansal, A.; Tan, M.X.; Tufts, B.J.; Lewis, N.S. *J. Phys. Chem.* **1993**, *97*, 7309.
21. Gu, Y.; Waldeck, D.H. *J. Phys. Chem.* **1996**, *100*, 9573.

About the Authors

Nathan S. Lewis received his B.S. and M.S. degrees from Caltech in 1977 and his Ph.D. from MIT in 1981. He is now a Professor of Chemistry and Principal Investigator in the Beckman Institute Molecular Materials Resource Center at Caltech. Lewis received the ACS Award in Pure Chemistry and the Fresenius Award for his work in the photochemical behavior of semiconducting electrodes. His address is Division of Chemistry and Chemical Engineering, California Institute of Technology, Pasadena, California 91125. Correspondence should be addressed to him.

Arnel M. Fajardo is a graduate student in the chemistry department at Caltech. He received his B.S. degree from Florida State University in 1993.

©Copyright 1997 by the Center for Photochemical Sciences
The Spectrum is a quarterly publication of the Center for Photochemical Sciences, Bowling Green State University, Bowling Green, OH 43403.
Phone 419-372-2033 Fax 419-372-6069
Email photochemical@listproc.bgsu.edu
WWW <http://www.bgsu.edu/departments/photochem/>

Executive Director: D.C. Neckers
Administrative Director: Pat Green
Principal Faculty: G.S. Bullerjahn, J.R. Cable,
K.D. Deshayes, Y.J. Ding,
W.R. Midden, M.V. Munschau,
D.C. Neckers, M.Y. Ogawa,
M.A.J. Rodgers, D.L. Snavelly

The Spectrum Editor: Pat Green
Production Editor: Alita Frater

COPYRIGHT PERMISSION

A person may make a single copy of any or all articles in this issue for personal use. Copying beyond that permitted by the U.S. Copyright law is allowed provided that the appropriate per copy fee is paid through the Copyright Clearance Center, Inc., 27 Congress St., Salem, MA 01970. For reprint permission, please write to the Center for Photochemical Sciences.

EDITORIAL POLICY

The Spectrum reserves the right to review and edit all submissions. The Spectrum is not responsible for contents of articles.

Articles submitted to The Spectrum will appear at the discretion of the editorial staff as space is available.

Collisional Deactivation of Large, Highly Vibrationally Excited Molecules

John R. Barker, Department of Atmospheric, Oceanic and Space Sciences
and Department of Chemistry, University of Michigan

Introduction

Recent work on large molecule vibrational energy transfer has focused on characterizing the collision step-size distribution...the distribution of energies transferred per collision. Why does it matter? Collisional energy transfer is of central importance in unimolecular decomposition, free radical recombination, the dissipation of vibrational excitation in laser-induced reactions, and in many other non-equilibrium chemical reaction systems. The collision step-size distribution provides, in its most general form, a complete description of energy transfer. Photochemistry offers many examples of non-equilibrium systems, and thus photochemistry and molecular energy transfer have been closely associated for many years. In fact, most energy transfer investigations have been carried out by exploiting photoexcitation techniques.

In this paper, we will describe some experimental and theoretical results obtained on large molecule energy transfer, but several recent reviews present more detailed descriptions of experimental techniques, data, and analysis.¹⁻⁷

Highly Vibrationally Excited Large Molecules

In a typical experiment, highly vibrationally excited molecules are produced by a laser pulse and then they are deactivated in a series of collisions. Each collision removes, or adds, vibrational energy and the collision partner may be left in a different internal energy state:



where excited molecule A has vibrational energy E, prior to the collision, and energy E', afterwards. The energy transfer step-size is the quantity (E'-E). The collider M will recoil with a new translational speed and, if it is non-monatomic, its rovibrational state may have changed.

All stable molecules have vibrational states. When those states are widely spaced, relative to their natural widths, energy transfer can be described as a state-to-state process. This limiting behavior corresponds to the sparse density of states (small molecule) limit. When the molecule is highly excited and has enough vibrational modes, the vibrational state density is so high that the states overlap to produce a quasi-continuum. This corresponds to the high density of states (large molecule) limit, in which intramolecular vibrational redistribution (IVR) is rapid. In this limit,

essentially every energy transfer step-size is possible, subject to conservation of energy and angular momentum. Vibrational energy transfer in the small molecule limit has been studied for many years and is well understood.⁸ Quantitative theories have been developed and applied to molecules as large as p-difluorobenzene, at low excitation energy.^{9,10} Large molecule energy transfer has been studied even longer than the small molecule variety, but only its qualitative features are known: no quantitative theories have been developed.

The vibrational state density for benzene is shown in Figure 1 as a function of total vibrational energy. At state densities less than ~ 100 states/cm⁻¹, the states are discrete and non-overlapping. For a natural line width corresponding to an infrared spontaneous emission rate of $\sim 10^3$ s⁻¹, the large molecule limit is reached when the state density is $\sim 10^7$ states/cm⁻¹. These limits are not very sharp, however. For many molecules, rapid IVR takes place when the average vibrational state density is of the order of 10^2 - 10^3 states/cm⁻¹, indicating that "large molecule"

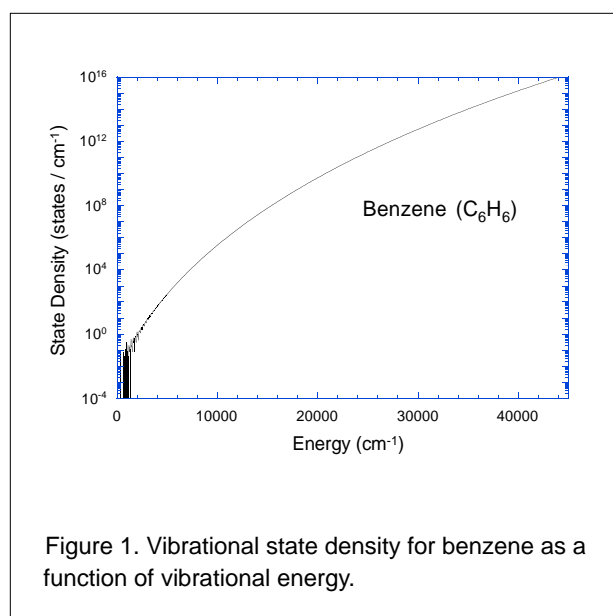
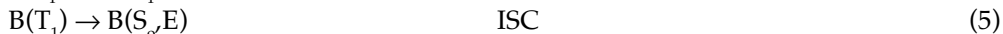
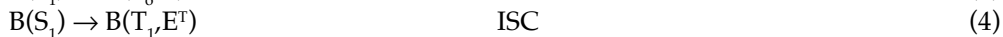


Figure 1. Vibrational state density for benzene as a function of vibrational energy.

behavior can occur even at these low state densities. This phenomenon may be due to clumps of states where the local vibrational state density is high.

In recent years, highly vibrationally excited molecules in the large molecule limit (HVEM's) have been prepared by using laser photoexcitation and subsequent radiationless transitions. We have employed this method to produce highly vibrationally excited azulene, benzene derivatives, and pyrazine in the electronic ground state.^{3,4,11} Other researchers have applied the same general approach to other systems in order to study energy transfer in the ground and excited electronic states.^{5,7} When benzene vapor is excited using a 248 nm pulsed laser, the initially prepared excited singlet state undergoes internal conversion (IC) and intersystem crossing (ISC) to produce the electronic ground state with vibrational energy E approximately equal to $h\nu$:



Here, S_0 , S_1 , and T_1 denote the singlet electronic ground state, the first excited singlet state, and the first excited triplet state, respectively; vibrational energy in the T_1 state is denoted E^T . For benzene excited at 248 nm, this process requires a small fraction of a microsecond. By controlling pressures in a suitable range, the process is complete before significant energy transfer takes place.

HVEM's can also be produced by direct vibrational overtone pumping.^{12,13} This method has the advantage that it does not require conveniently situated excited electronic states and rapid radiationless transitions, but the absorption cross section is very small and the process produces only very low instantaneous concentrations of the HVEM's. Usually, the technique is applied to chemical reaction systems, where reaction products are measured, and energy transfer is measured in competition with the chemical reaction. This technique is very useful for investigating both energy transfer and unimolecular reaction rates. For detailed energy transfer studies, however, direct detection of the HVEM's is desirable in order to avoid potential complications from side reactions.

HVEM's in the electronic ground state are difficult to detect directly and, hence, energy transfer is difficult to measure. In our laboratory, we have used time-resolved spontaneous infrared fluorescence (IRF) from the C-H and C-D emission bands of the excited molecules, because the IRF intensity is related in a simple way to the total vibrational energy.^{3,4,11} In a typical experiment, we use a pulsed 248 nm laser to excite the gas and we observe the IRF with a band-pass filter and an InSb semiconductor detector. Other researchers have employed time-resolved FTIR spectroscopy to monitor spectral shifts and from them deduce the excitation energy.^{5,7} Still other groups have very productively used time-resolved ultraviolet absorbance and multiphoton ionization to probe the HVEM's.⁷

Instead of probing the HVEM's, themselves, an alternative approach is to monitor formation of energy transfer products. HVEM's can produce vibrationally excited CO_2 , which emits spontaneously in the infrared, *via* vibration-to-vibration (V-V) energy transfer. Flynn and coworkers have used tunable diode laser (TDL) absorption spectroscopy to monitor the production of individual rovibrational states and to measure Doppler shifts due to the translational energy release which accompanies vibrational and rotational quantum number changes (i.e. V-V/T/R energy transfer).^{6,14} This powerful technique has produced valuable insights into the dynamics of energy transfer collisions.

The V-T/R Collision Step-Size Distribution, $P(E', E)$

When the collider gas is monatomic, a large excited molecule is deactivated only *via* vibration-to-translation and rotation (V-T/R) energy transfer. For V-T/R energy transfer, the step-size distribution should be interpreted as follows: $P(E', E)dE'$ is the probability that after a single collision, a molecule with initial energy E will be found in the energy range E' to $E'+dE'$. Historically, it was assumed that for a large molecule every collision produces an energy change and therefore that $P(E', E)$ is normalized: every collision is inelastic. This assumption was made, because a quasi-continuum of vibrational energy levels exists (in the large molecule limit) and therefore one can argue that it is unlikely that any collision would be elastic. As will be shown below, it is possible that this assumption is not valid.

One general property of the collision step-size distribution derives from first principles: the probabilities of activation and deactivation are related through detailed balance. For a thermal energy distribution, there is a significant chance that any given collision will further activate the already excited molecule. It is useful to describe energy transfer just in terms of the deactivating collisions, since we can determine the rate of activation by using the detailed balance relationship. Thus, we distinguish between $P(E', E)$, which applies to all collisions, and $P_d(E', E)$, which only applies for deactivation ($E' \leq E$).

Experimental Determinations of $P(E',E)$

The collision step-size distribution has never been measured directly, but many of its properties can be inferred from the experimental techniques mentioned above. From IRF experiments, for example, we determine the average amount of energy transferred in the average collision, $\langle\Delta E(E)\rangle$. This average step-size depends on excitation energy, temperature, and other variables, and it includes both activating and deactivating collisions. By making simple assumptions about the functional form of $P(E',E)$, we can determine the average energy transferred in just the deactivating collisions, $\langle\Delta E(E)\rangle_d$.

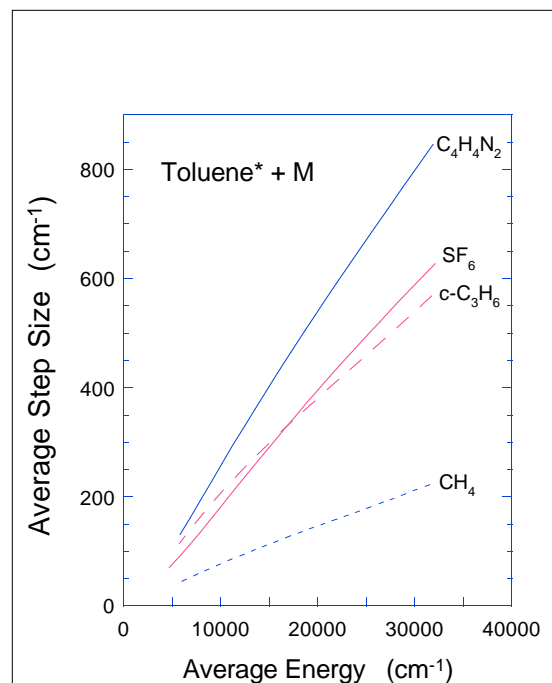


Figure 2. Average magnitude of $\langle\Delta E\rangle$ as a function of average energy, for the deactivation of excited pyrazine by several collider gases.¹⁶

For purposes of mathematical convenience and with some support from chemical activation experiments, $P_d(E',E)$ has often been approximated by an exponential function:¹⁵

$$P_d(E',E) = c(E) \exp [-(E - E')/\alpha(E,T)], \quad (6)$$

where $c(E)$ is a normalization factor. This "exponential model" contains the empirical parameter $\alpha(E,T)$, which is approximately equal to $\langle\Delta E(E)\rangle_d$ and depends on excitation energy, temperature, and the identity of the collision pair. Our IRF data^{3,4,11} show that $\langle\Delta E(E)\rangle$, $\langle\Delta E(E)\rangle_d$ and $\alpha(T,E)$ have very little dependence on temperature, but all are almost directly proportional to vibrational energy, as shown in Figure 2 for $\langle\Delta E(E)\rangle$ obtained for the deactivation of excited pyrazine.¹⁶ In some applications, the exponential model provides an adequate description. Single-channel unimolecular reactions do not depend sensitively on the details of the step-size distribution, but multi-channel reaction branching ratios are determined by the shape of $P(E',E)$.^{17,18}

A little more than ten years ago, Oref, Steele, and coworkers found experimentally that the probability of large step-sizes is much greater than predicted by the exponential model.¹⁹ They concluded that this enhanced energy transfer was due to "supercollisions". Essentially, however, the phenomenon of "supercollisions" merely describes the deviations from the exponential model. Since the exponential model has no firm fundamental justification, deviations are to be expected.

In a series of elegant experiments using multiphoton ionization, Klaus Luther and coworkers detected the HVEM's as they were being deactivated in the collisional cascade.²⁰ A small population appeared very quickly in a "window" of low energies, showing that

some collisions are extremely efficient, while most of the collisions had more modest efficiencies. The data were interpreted in terms of a biexponential model:

$$P_d(E',E) = c(E) \{ (1-f_c) \exp [-(E - E')/\alpha(E,T)] + f_c \exp [-(E - E')/\beta(E,T)] \}, \quad (7)$$

where f_c is a small fraction, $\beta(E,T)$ is an empirical parameter, and the other factors were defined above. In their most recent work, Luther and coworkers have proposed another empirical functional form, which requires fewer parameters:

$$P_d(E',E) = c(E) \exp \{ -(E - E')/\alpha(E,T)^b \}, \quad (8)$$

where b is an empirical parameter.

In our own laboratory, we also found that the exponential model requires an extension. By using IRF data from two infrared bands (the C-H fundamental and overtone), we determined both the mean value and the width of the time-dependent energy distribution.⁴ The width is particularly sensitive to details of the collision step-size distribution, and we used a biexponential distribution to fit the data. Master equation simulations of the experiment show how the population distributions start from the initial narrow energy distribution, how they broaden, how they cascade down the energy ladder, and how they stack up at low energy to regenerate the Boltzmann distribution. These effects are illustrated for pyrazine deactivation²¹ in Figure 3.

In all of the empirical expressions for $P_d(E',E)$ deduced from experiments, the parameter $\alpha(E,T)$ is also nearly independent of temperature and approximately directly proportional to energy. For comparison, Figure 4 depicts the three empirical step-size distribution functions deduced in two different experiments^{3,20} for the deactivation of

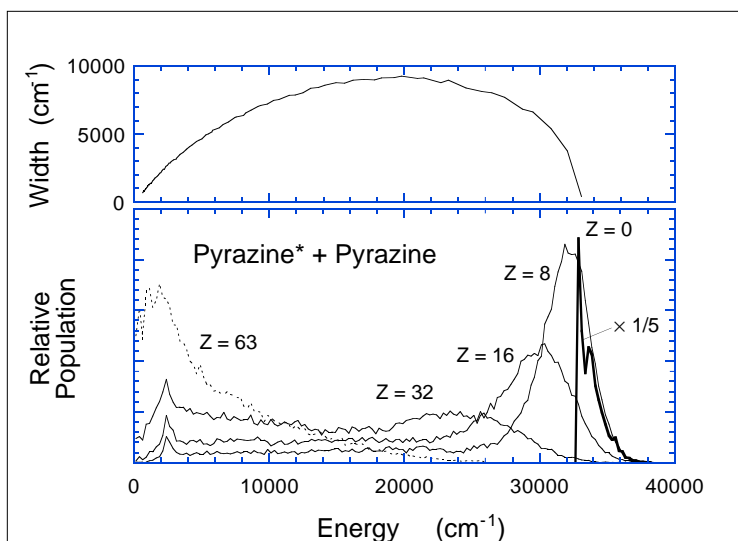


Figure 3. Master equation simulations which match the experimental data for deactivation of excited pyrazine by unexcited pyrazine.²¹ The average width of the population distribution first increases and then decreases, during the collisional cascade.

are qualitatively in agreement with the empirical expressions and the technique shows promise as a quantitative method for obtaining $P(E',E)$ in systems where the TDL technique is applicable. We and other workers are investigating molecular beam techniques for directly obtaining $P(E',E)$, but no results have been reported, as yet.

Theoretical Determinations of $P(E',E)$ for V-T/R/R Transfer

Theory has lagged seriously behind experiment for energy transfer involving HVEM's. Classical trajectory calculations currently provide the most generally useful theoretical approach for studying large molecule energy transfer.^{7,22,23,24} These studies provide qualitative insight and even semi-quantitative agreement with experiments. For example, trajectory calculations predict step-size distributions which resemble the bi-exponential model, but it is not

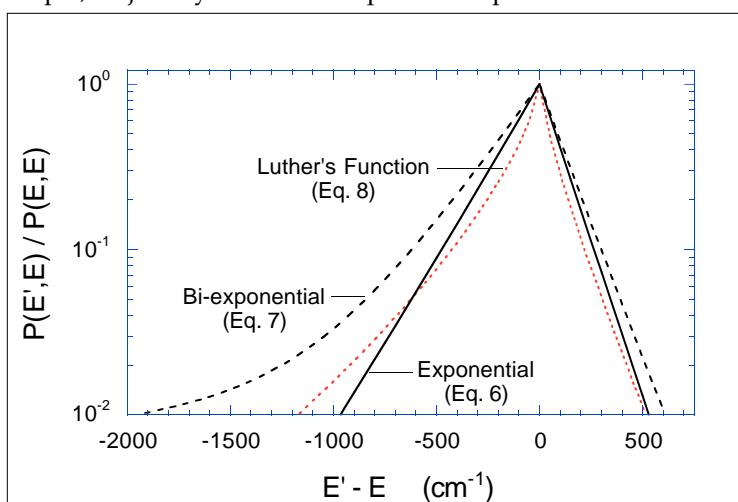


Figure 4. Empirical models for the collision step-size distribution, $P(E',E)$, for toluene (with $E = 20,000 \text{ cm}^{-1}$) deactivated by argon. Note that down-steps are favored and that $\langle \Delta E \rangle$ is averaged over both up- and down-steps, while $\langle \Delta E \rangle_d$ is averaged only over down-steps.

excited toluene by argon. The agreement among the three curves is very good. The differences among the curves partly reflect the differences between the experiments and the effects of experimental uncertainties. The deviations from the exponential model are difficult to detect and therefore relatively uncertain. According to the conventional view, the energy dependence of $\langle \Delta E(E) \rangle$ is explained by making $\alpha(E,T)$ larger at higher energies, and thus the "wings" of the distributions will extend to higher and lower energies. However, it should be emphasized once again that the expressions for $P_d(E',E)$ are empirical, they are assumed to be normalized, and they have little theoretical foundation.

As mentioned above, an important advance in the experimental determination of $P(E',E)$ for V-V/T/R energy transfer has been made by Flynn and coworkers, who use TDL spectroscopy to measure quantum state resolved production of $\text{CO}_2(v_1 v_2 v_3 J)$ produced in collisions with HVEM's.^{6,14} By making judicious assumptions, they have analyzed their data to obtain segments of $P_d(E',E)$. The results obtained so far

are qualitatively in agreement with the empirical expressions and the technique shows promise as a quantitative method for obtaining $P(E',E)$ in systems where the TDL technique is applicable. We and other workers are investigating molecular beam techniques for directly obtaining $P(E',E)$, but no results have been reported, as yet.

clear whether this success is due to an accidental cancellation of errors.

Classical trajectory calculations may suffer from several deficiencies, due to differences between classical and quantum mechanics, but the quantitative importance of these deficiencies is not yet known.³ The most obvious deficiency is that zero point energy is not conserved in classical mechanics. When the zero point energy is not conserved, several non-physical effects can lead to erroneous predictions. The non-conserved zero point energy may erroneously enhance predicted energy transfer and it can even falsely contribute to predicted bond dissociation when the energy ought to be insufficient for bond breakage. A more subtle deficiency is that, unlike classical systems, quantum systems do not exhibit equipartition of energy. Quantitative comparisons between classical and quantum mechanics are currently being carried out by Schatz and Lendvay on prototype energy transfer systems.²⁵

In our own laboratory, we are developing a statistical-dynamical theory which we hope can describe both small and large molecule energy transfer over a very wide range of excitation energies.²⁶ The theory is necessarily approximate and it may have only limited predictive capabilities, but it will provide an alternative to classical trajectory calculations. In Figure 5 we present calculated collision step-size distributions for cyclopropane deactivation by helium at room temperature.

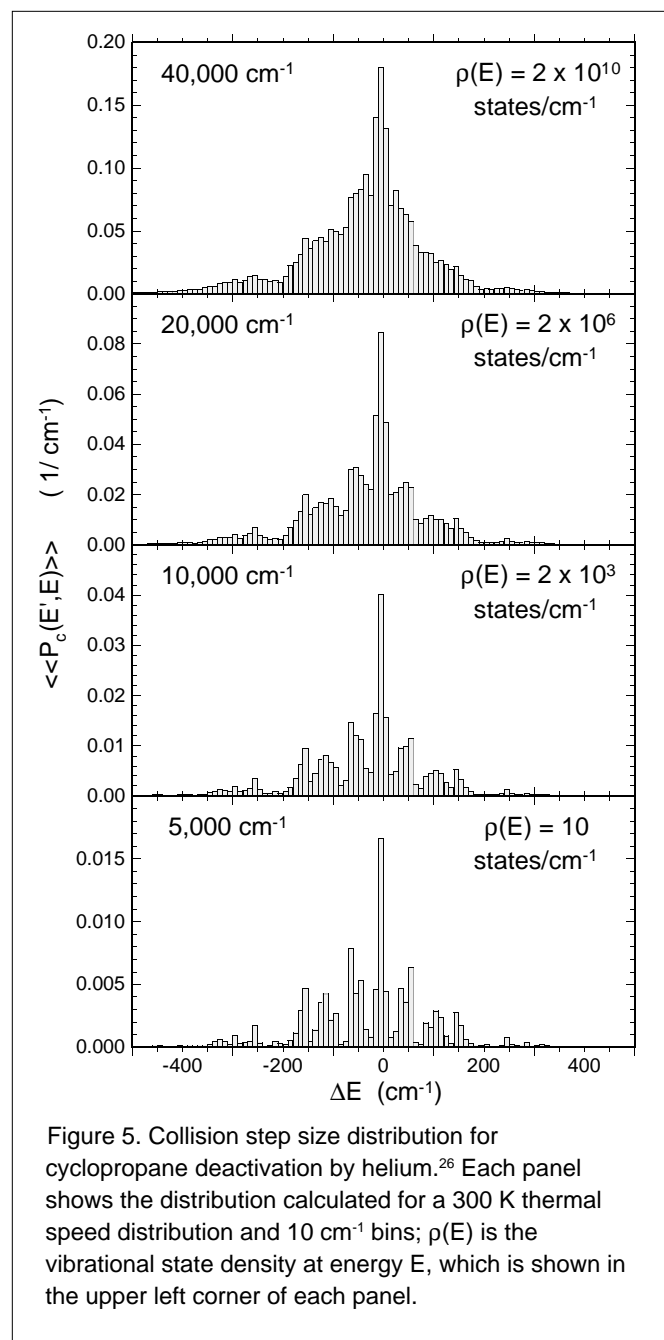


Figure 5. Collision step size distribution for cyclopropane deactivation by helium.²⁶ Each panel shows the distribution calculated for a 300 K thermal speed distribution and 10 cm^{-1} bins; $\rho(E)$ is the vibrational state density at energy E , which is shown in the upper left corner of each panel.

One of the most striking properties of the calculated step-size distributions in Figure 5 is the presence of energy transfer "propensities", in which transitions with almost equal values of ΔE have significantly different probabilities. Energy transfer propensities have been measured experimentally in large molecule energy transfer at low energies, where the states can be optically resolved (4,39), but never at high energies. The calculated energy transfer propensities are at least partially preserved even at energies as high as 40,000 cm^{-1} , although they are "smeared out" by anharmonicity. The present theory is based on separable vibrational modes and we do not yet know whether the propensities would be as distinct if inter-mode interactions were included.

A second striking property is that the envelope of $P(E',E)$ is roughly similar to the empirical distributions, but the width does not change significantly with energy. Instead, the probability amplitude varies. This result is in agreement with the experimental finding that $\langle\Delta E(E)\rangle$ varies with internal energy, but it is in strong contrast with the usual assumption that every collision is inelastic. Instead, it predicts that the proportion of inelastic collisions varies with energy, as is certainly the case in the small molecule limit.

The statistical-dynamical theory presented here shows promise for calculating the collision step-size distribution function needed for master equation calculations and predicting unimolecular reaction rate constants in the fall-off regime. It is useful even at energies where densities of states are greater than 10^{10} $\text{states}/\text{cm}^{-1}$. However, the theory still requires further testing and verification, and any conclusions must be tempered with caution.

Conclusions

In summary, the study of large molecule energy transfer is in a state of flux: better experimental techniques are being brought to bear and better theoretical descriptions are being developed, but there is much room for further improvement. Although our current view of the phenomenon is still cloudy, we expect the situation to improve greatly in the next few years. It will be very satisfying to be able to make accurate quantitative predictions of energy transfer in non-equilibrium systems.

Acknowledgments

I am very grateful for my interactions over the years with the members of my group and other colleagues. In particular, I wish to acknowledge the following individuals for their direct scientific contributions and for the many stimulating conversations regarding energy transfer: Keith D. King, Beatriz M. Toselli, Jichun Shi, Jerrell D. Brenner,

Alexander Chimbayo, and Laurie M. Yoder. My thanks go to the Department of Energy, Office of Basic Energy Sciences, for partial financial support of the work described here.

References

1. Hippler, H.; Troe, J. In *Bimolecular Collisions*; Baggott, J.E.; Ashfold, M.N., Eds.; The Royal Society of Chemistry: London, 1989; p 209.
2. Oref, I.; Tardy, D.C. *Chem. Rev.* **1990**, *90*, 1407.
3. Barker, J.R.; Toselli, B.M. *Int. Rev. Phys. Chem.* **1993**, *12*, 305.
4. Barker, J.R.; Brenner, J.D.; Toselli, B.M. *Adv. Chem. Kin. Dyn.* **1995**, *2B*, 135.
5. *Vibrational Energy Transfer Involving Large and Small Molecules*; Barker, J.R., Ed.; *Adv. Chem. Kin. Dyn.* **1995**, *2A, 2B*.
6. Flynn, G.W.; Parmenter, C.S.; Wodtke, A.M. *J. Phys. Chem.* **1996**, *100*, 12817-12838.
7. *Ber. Bunsenges. Phys. Chem.* **1997**, *101* (3), Special Issue on *Unimolecular Reactions*, Crim, F.F.; Troe, J., Eds.
8. Yardley, J.T. *Introduction to Molecular Energy Transfer*; Academic Press: New York, NY, 1980.
9. Clary, D.C. *J. Phys. Chem.* **1987**, *91*, 1718-1727.
10. Clary, D.C.; Kroes, G.J. *Adv. Chem. Kin. Dyn.* **1995**, *2A*, 135.
11. Barker, J.R. *J. Phys. Chem.* **1984**, *88*, 11.
12. Snively, D.L.; Zare, R.N.; Miller, J.A.; Chandler, D.W. *J. Phys. Chem.* **1986**, *90*, 3544.
13. Snively, D.L.; Grinevich, O.; Hassoon, S.; Snively, G. *J. Chem. Phys.* **1996**, *104*, 5845.
14. Flynn, G.W.; Weston, R.E., Jr. *Adv. Chem. Kin. Dyn.* **1995**, *2B*, 359.
15. Tardy, D.C.; Rabinovitch, B.S. *Chem. Rev.* **1977**, *77*, 369.
16. Miller, L.A.; Barker, J.R. *J. Chem. Phys.* **1996**, *105*, 1383.
17. Gilbert, R.G.; Smith, S.C. *Theory of Unimolecular and Recombination Reactions*; Blackwell Scientific Publications: Oxford, 1990.
18. Baer, T.; Hase, W.L. *Unimolecular Reaction Dynamics: Theory and Experiments*; Oxford University Press: Oxford, 1996.
19. Oref, I. *Adv. Chem. Kin. Dyn.* **1995**, *2B*, 285.
20. Hold, U.; Lenzer, T.; Luther, K.; Reihls, K.; Symonds, A. *Ber. Bunsenges. Phys. Chem.* **1997**, *101*, 552.
21. Miller, L.A.; Cook, C.D.; Barker, J.R. *J. Chem. Phys.* **1996**, *105*, 3012.
22. Brown, N.; Miller, J.A. *J. Chem. Phys.* **1980**, *80*, 5568-5580.
23. Gilbert, R.G. *Int. Rev. Phys. Chem.* **1991**, *10*, 319.
24. Lendvay, G.; Schatz, G.C. *Adv. Chem. Kin. Dyn.* **1995**, *2B*, 481.
25. Lendvay, G.; Schatz, G.C. *Ber. Bunsenges. Phys. Chem.* **1997**, *101*, 587.
26. Barker, J.R. *Ber. Bunsenges. Phys. Chem.* **1997**, *101*, 566.

About the Author

Dr. Barker received his Ph.D. in chemistry at Carnegie Mellon University and is a professor in the Department of Chemistry and the Department of Atmospheric, Oceanic, and Space Sciences at the University of Michigan, Ann Arbor, Michigan 48109-2143.

Time Resolved ESR and CIDNP Spectroscopy: Two Versatile Tools for the Investigation of Photoinitiators

Kurt Dietliker, David Leppard, Ciba Specialty Chemicals Inc., Marly, Switzerland;

Martin Kunz, Ciba Specialty Chemicals Inc., Basel, Switzerland;

Iwo Gatlik, Urszula Kolczak, Piotr Rzadek, and Günther Rist, Novartis Services AG, Basel, Switzerland

Introduction

The outstanding advantages of radiation curing in terms of economy, ecology and product quality relative to thermal curing processes are well-known and have led to fast acceptance of this technology in many industrially important applications. For example, this process is the basis of most photoimaging processes which are used in the printing and electronics industry.^{1,2}

The photoinitiator is a key compound in all light curable formulations and is responsible for the transformation of light into chemical energy. The introduction of new raw materials and light sources, the development of novel applications as well as new legal regulations continuously impose new requirements on photoinitiators. Hence, the development of photoinitiators with properties which meet industrial needs is a continuous challenge.

The understanding of the photochemistry and the initiation processes is the basis for the rational design of new photoinitiators with improved reactivity. Furthermore, the knowledge of all reaction channels and the products formed therefrom is an integral part of the assessment of photoinitiators.

A wide variety of experimental methods are available for the investigation of photochemical reactions. Electron spin resonance (ESR) and chemically induced nuclear polarization (CIDNP) spectroscopy are two powerful techniques which have been successfully used in our laboratories for studies of photoinitiators and initiation processes involving radical reactions.³⁻⁶

The following paragraphs illustrate with applications from our laboratories how these methods can be used to study industrial photoinitiators and provide important information for the development of new initiators. Emphasis is given to time-resolved experiments which allow to follow the evolution of radicals and products over time.

Time-resolved ESR and CIDNP Spectroscopy

A number of spectroscopic methods are available for the study of photochemical reactions. Time-resolved laser flash spectroscopy, which allows the observation of transients and intermediates by their absorption in the UV/visible or infrared is a commonly used method. While this technique allows a high time resolution, up to the femtosecond range, the information obtained on the structure of the species observed is very limited.

The strength of magnetic resonance for the investigation of radicals and radical reaction products lies in its inherently high resolution, the ability to follow structural changes during radical photoreactions, and the possibility to observe the resulting photoproducts immediately after formation. Although time resolution is lower than for optical methods, the continuous development of the experimental techniques and instrumental hardware now allows time resolution in the nanosecond range (50-100 nsec). This is adequate for the observation of most radical reactions occurring during the photoinitiation process.

Time-resolved ESR spectroscopy (TR-ESR)

Time-resolved ESR (TR-ESR) is a powerful tool for the investigation of unstable radicals. If radicals are formed in pairs and strong electron spin polarization is built up either by the triplet or radical pair mechanism, continuous microwave experiments are the easiest approach to characterize the transient radicals. Usually these experiments are performed with a pulsed Nd-YAG laser or an equivalent light source at a fixed magnetic field without field modulation. This technique is described in detail in references 7 and 8.

In these TR-ESR experiments, the time dependence of the magnetization after a light pulse of a few nanoseconds is stored in a fast digital storage oscilloscope at a constant magnetic field. This experiment is repeated many times at this and other field settings. All the experimental traces thus obtained represent a three-dimensional picture of the magnetization as a function of time and magnetic field. Integration over certain time intervals leads to TR-ESR spectra of the transient radicals, which in most cases can be unequivocally assigned to chemical structures.

The time resolution of this technique is limited to 50-100 ns by the available electronic equipment and the time needed for the build-up of the magnetization of the newly formed radicals in the microwave field.

Time-resolved CIDNP (TR-CIDNP)

In CIDNP experiments, the nuclear spin polarization of products formed from radical pairs, either by recombination or disproportionation within the primary solvent cage or by escape reactions, is observed. These reactions are nuclear spin dependent and the two pathways act as a chemical switch which channels different nuclear spin configurations to either escape or cage products. This channeling effect leads to emission and enhanced absorption in the NMR-spectra of the products.⁹⁻¹⁰

As for ESR spectra, the time dependence of the nuclear spin polarization can be recorded in time-resolved CIDNP (TR-CIDNP) experiments. The maximum time resolution is similar to ESR and is limited by the width of the radio frequency pulse.

The results obtained from TR-ESR and CIDNP spectroscopy are complementary, since radicals are directly observed by the first method, while the products formed from radical precursors prior to nuclear spin relaxation can be investigated by the second technique.

Sensitization of α -Amino Ketones

The sensitivity of many photoinitiators can be considerably improved by sensitization. A typical example is the 2.5 fold increase in curing efficiency observed when the α -amino ketone photoinitiator, 2-methyl-1-[4-(methylthio)phenyl]-2-morpholinopropan-1-one **1**, is used in combination with isopropylthioxanthone **2** in a highly pigmented blue silk screen printing ink.⁵

The reactivity enhancement is due to the fact that the thioxanthone has a longer wavelength absorption ($\lambda_{\max} \approx 380$ nm) than the initiator, which allows for better use of the light not absorbed by the pigment. The sensitizer can then transfer the energy to the shorter wavelength absorbing α -amino ketone. The improvement is highest at relatively high film thicknesses or in highly pigmented systems, where the light screening effect of the pigment is most pronounced. Under these conditions the photoinitiator is activated by interaction with the excited state sensitizer.

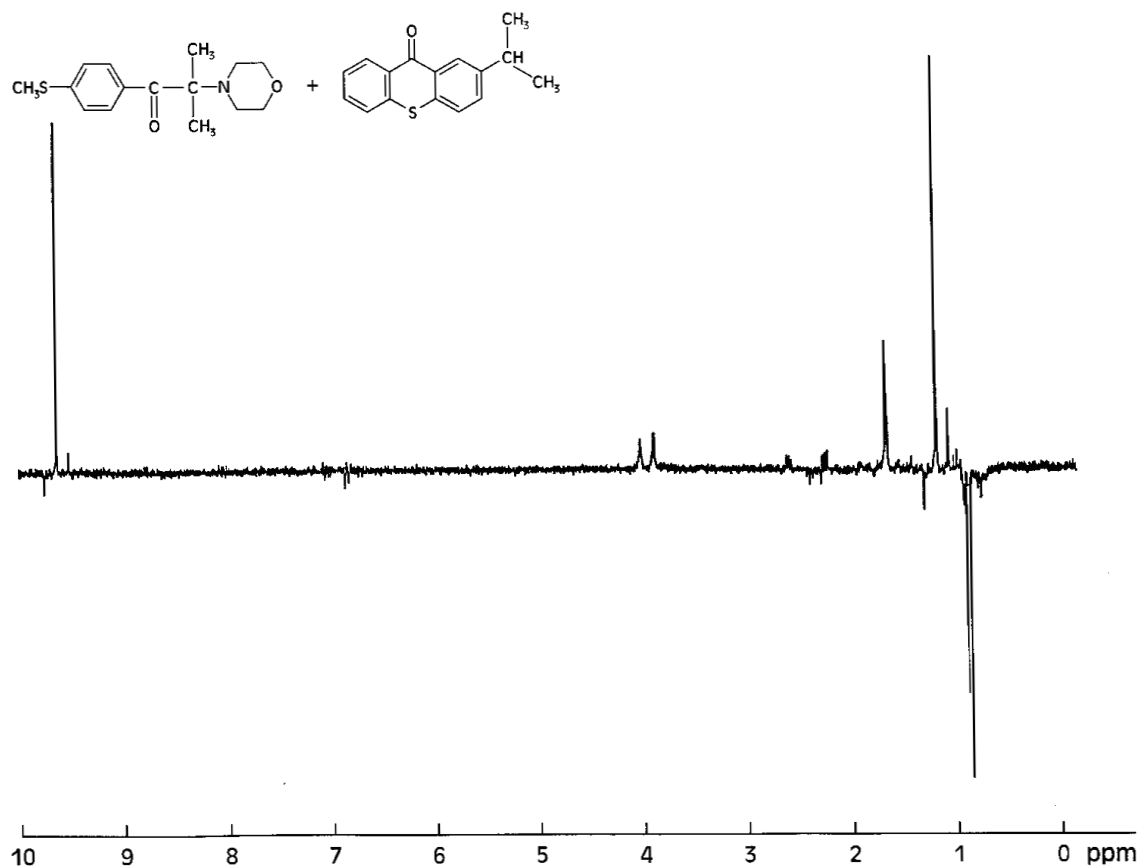


Figure 1. Time-resolved ^1H -NMR CIDNP spectrum of an irradiated sample of **1** and **2** in benzene.

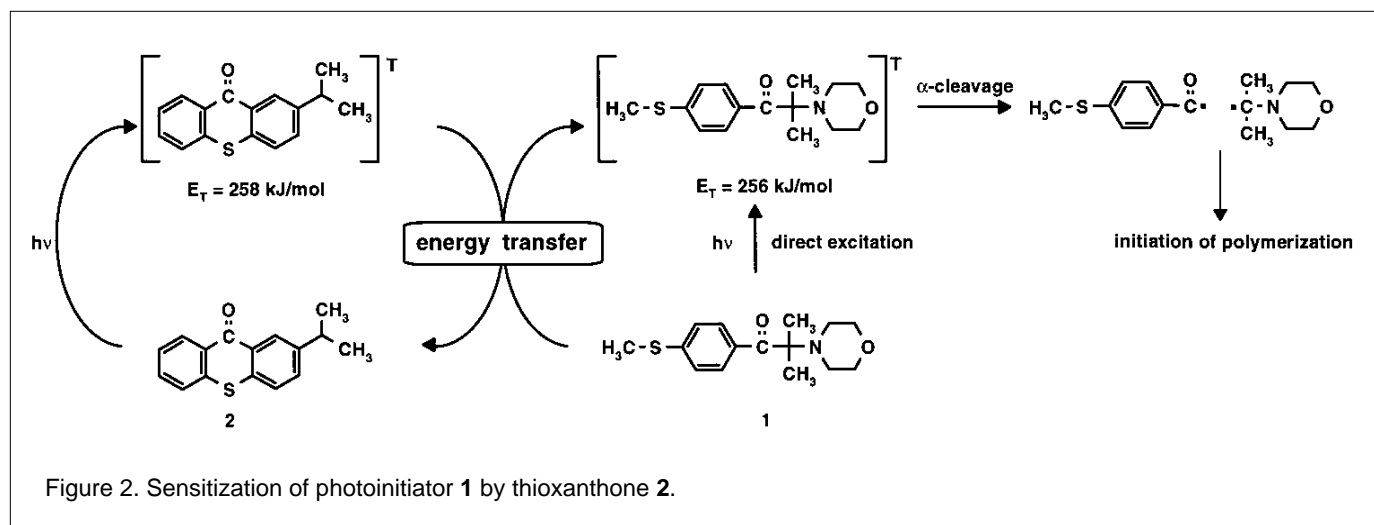
Although the improvement of reactivity for a technical application is of importance regardless of the mechanism causing the synergistic effect, the understanding of this effect is crucial in view of the continuing effort to improve photoinitiator efficiency.

The sensitization process was studied using both ESR- and CIDNP⁵ experiments. Due to its high resolution, time-resolved CIDNP spectroscopy turned out to be the more adequate technique to elucidate this particular chemical reaction, and this method seems to be, well suited for studying sensitization processes leading to radical pairs.

TR-CIDNP spectra were obtained upon irradiation of a mixture of the α -aminoketone photoinitiator **1** and isopropylthioxanthone **2** in benzene. The spectrum of Figure 1 was obtained with a carefully degassed sample approximately 1 μ s after the pulse of a dye-laser emitting at 404.5 nm.

At this wavelength, only the thioxanthone **2** absorbs sufficient light to undergo efficient photochemical reactions. The NMR-resonances in Figure 1 are typical for the α -cleavage of photoinitiator **1**. The spectrum shows the resonances associated with the reaction products of a substituted benzoyl and an α -aminoalkyl primary radical pair. The strong signal at 9.64 ppm vs. TMS (enhanced absorption) is due to the aldehyde proton of 4-methylthio-benzaldehyde formed in an in-cage disproportionation reaction. The second product of this reaction exhibits resonances at 3.98, 3.86 ppm and 1.68 ppm, which can be attributed to the two olefin protons and the methyl group of 2-morpholino propene. The polarizations of these signals are the same as in experiments where the initiator is directly excited, and are proof for the triplet spin character of the radical pair affording these products.

This spectrum, together with other CIDNP spectra obtained with whole series of similar ketones,⁵ is proof for sensitization via triplet energy transfer from the thioxanthone to the photoinitiator in an apolar medium (Figure 2). The triplet character of the precursor is expected, since thioxanthone **2** is known to undergo efficient intersystem crossing to the triplet state after excitation.



While no polarized signals stemming from the thioxanthone were observed in this CIDNP spectrum, such signals were indeed detected when the experiment was performed in a more polar solvent (methanol). The formation of ketyl radicals occurs under these conditions, indicative for a second competing reaction pathway in polar medium involving electron transfer.⁵

Acylophosphine Oxides

CIDNP experiments

Acylophosphine oxides are highly efficient photoinitiators for the curing of thick pigmented coatings. Monoacylophosphine oxide (MAPO) were discovered several years ago.^{11,12} Recently, the more efficient bisacylophosphine oxides (BAPO) were introduced as commercial products,^{13,14} and the use of trisacylophosphine oxides (TAPO) as photoinitiators has also been reported.¹⁵

Several investigations of the photochemistry of MAPO^{16,17} and BAPO photoinitiators⁶ have been published. Detailed studies of the photochemistry and structure-activity relationships resulted in the design of new bisacylophosphine oxides with improved reactivity.¹⁸

Here again, CIDNP spectroscopy served as an excellent tool for the study of the products obtained by cage and escape reactions of acylphosphine oxides. TR-ESR and ESR experiments are suitable techniques to study the initiator radicals and the first addition step in the initiation process.

A typical ^{31}P -CIDNP spectrum, obtained upon irradiation of the new photoinitiator bis(2,4,6-trimethylbenzoyl)-phenyl-phosphine oxide **4** in acetonitrile, is shown in Figure 3.

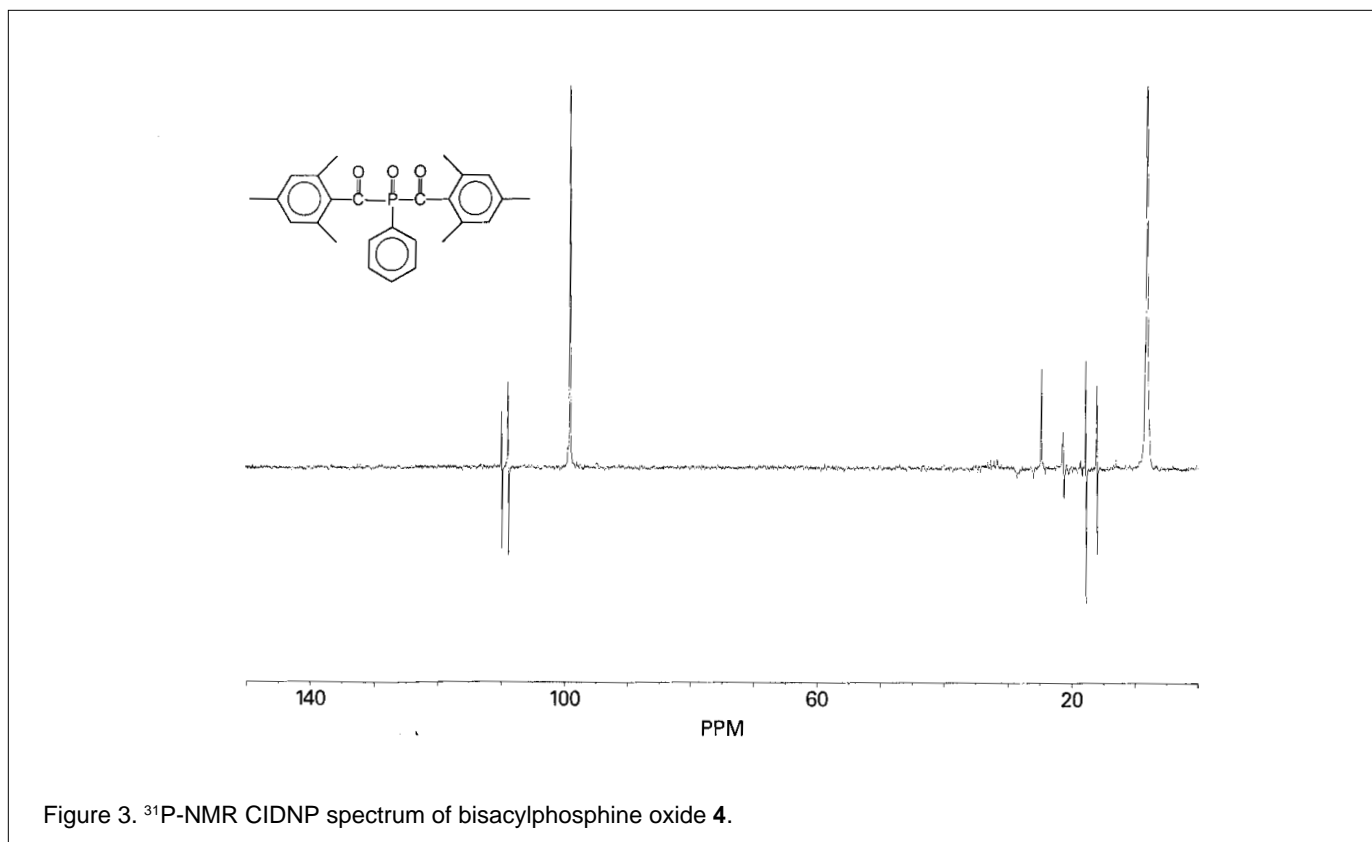


Figure 3. ^{31}P -NMR CIDNP spectrum of bisacylphosphine oxide **4**.

The phosphorus nuclear spin of pentavalent phosphorus oxides resonates between 0 and 50 ppm, while the resonances of trivalent phosphorus are observed at lower field strength (approximately 100-130 ppm). Products in both regions are observed for compound **4** and for other acyl phosphine oxides investigated.

As mentioned above, the radicals obtained by the photoinduced cleavage can re-encounter after diffusion and participate in both recombination and disproportionation reactions. In contrast to α -amino acetophenone photoinitiators such as **1**, disproportionation is a negligible reaction for the primary radicals of acylphosphine oxides even in structures where β -abstraction from an alkyl substituent on phosphorus is possible. In the absence of a trapping agent, recombination processes dominate. The most efficient reaction is the recombination affording the starting material (Figure 4). This process is manifested by the strong enhanced absorption at 7.92 ppm. Analysis of the polarization pattern reveals that the primary photochemical reaction is cleavage of the carbon-phosphorus bond of these bisacylphosphine oxides in their excited triplet state (α -cleavage).

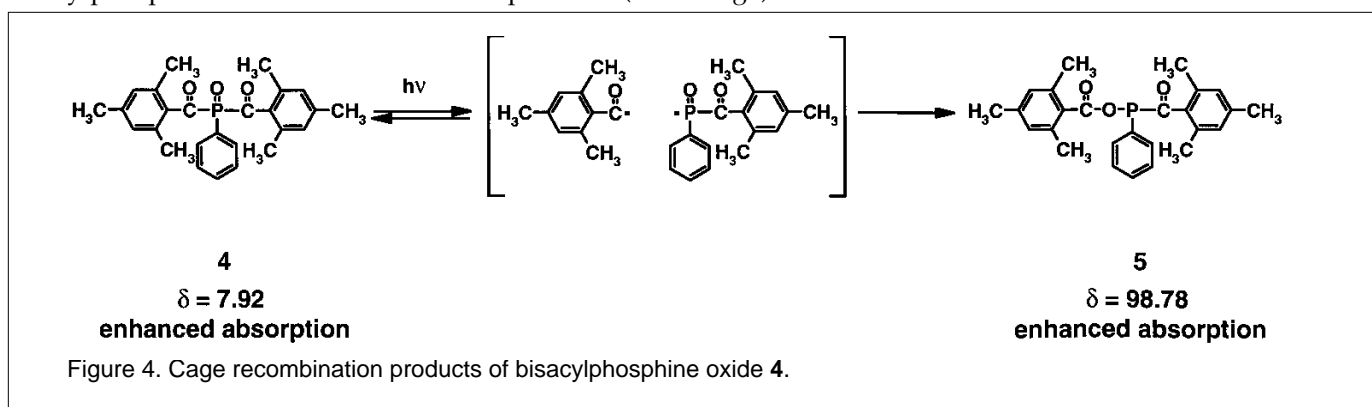
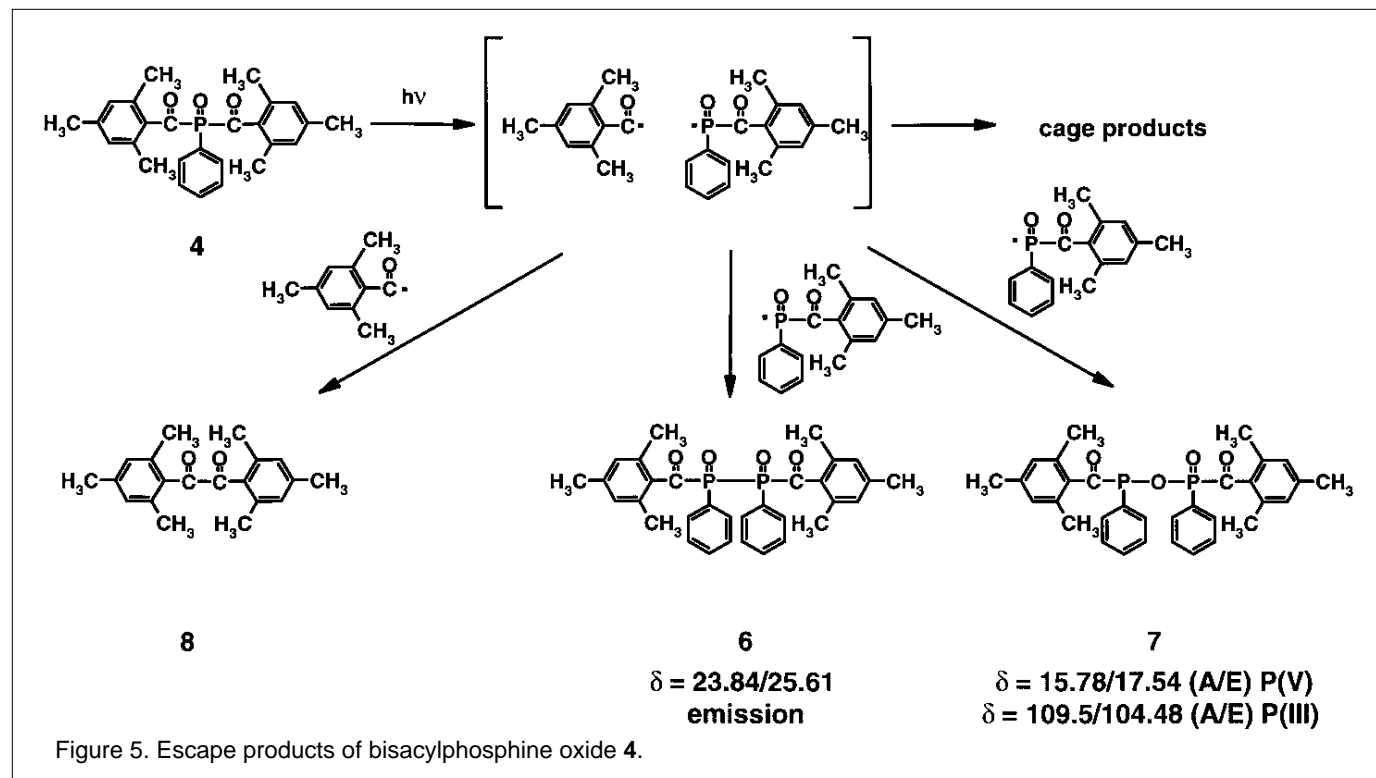


Figure 4. Cage recombination products of bisacylphosphine oxide **4**.

A second resonance at 98.78 ppm, exhibiting positive polarization must arise from a trivalent phosphorus atom in a product produced in a cage recombination process. This resonance line is assigned to compound 5, which arises by reaction of the benzoyl radical with the oxygen atom of its phosphinoyl radical counterpart (Figure 4). Such recombination reactions, which were observed for all mono- and bisacylphosphine oxides investigated, are good evidence that significant spin densities are found both on the phosphorus and oxygen atom in phosphinoyl radicals.

When the primary radicals leave the solvent cage and react with other radicals, escape products are formed (Figure 5). Whereas compounds formed from phosphorus radicals can be detected by ^{31}P -CIDNP spectroscopy, other methods such as ^{13}C - or ^1H -NMR-CIDNP are required to detect products which do not contain phosphorus (e.g. 8).⁶



Two dimers, one with a P-P bond (compound 6) and one with a P-O bond (compound 7) were observed in the ^{31}P -CIDNP spectrum. The asymmetric phosphorus atoms in these structures give rise to two pairs of diastereomeric compounds. The resonance signals at 23.84 and 25.61 ppm are due to the pentavalent phosphorus atoms in the diastereomers of compound 6.

In contrast to compound 6, the two phosphorus atoms in compound 7 are not magnetically equivalent and a ^{31}P - ^{31}P spin coupling is thus observed. This coupling gives rise to signals with doublet structure. The resonances at 15.78 and 17.54 ppm are attributed to the pentavalent phosphorus, those at 104.48 and 109.5 ppm to the trivalent phosphorus in 7. Both the emission type polarization of the resonances of 6 and the A/E (enhanced absorption/emission) multiplet polarization observed for 7 are in agreement with Kaptein's rules, which predict that signals of the escape products carry opposite polarization with respect to the cage recombination products.

The same type of resonances were observed upon irradiation of MAPO and TAPO photoinitiators. For BAPO⁶ and TAPO compounds, additional CIDNP experiments in the presence of a nitroxyl radical (TEMPO) as trapping agent gave evidence for two, respectively three stepwise photoinduced α -cleavages occurring after trapping of the phosphinoyl radicals.

Initiation process studied by ESR and TR-ESR

ESR spectroscopy allows direct observation of radicals formed upon irradiation of a photoinitiator. Figure 6 shows the TR-ESR spectrum of the BAPO initiator 4 obtained after irradiation with a single laser pulse (Nd-YAG laser, $\lambda = 355$ nm) in a toluene solution. Resonances of the two primary radicals are easily distinguished: The single line with a g-value of 2.0002 in the center of the spectrum is characteristic for the benzoyl radical. The resonances of the phosphinoyl radical form a doublet with a phosphorus hyperfine coupling constant of 25.9 mT and a g-value of 2.0038.

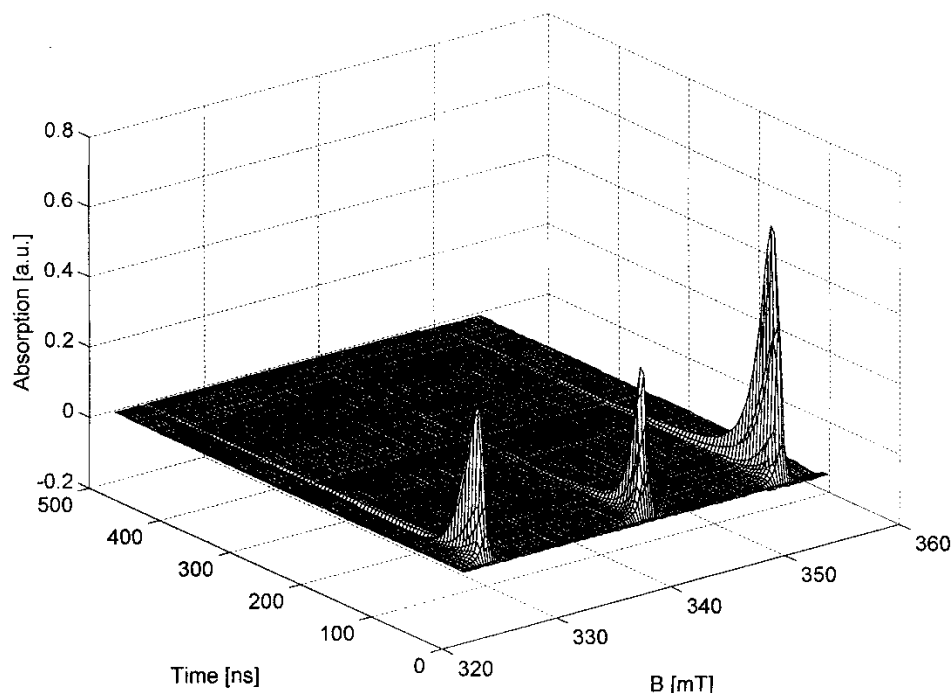


Figure 6. Time-resolved ESR spectrum obtained upon irradiation of BAPO 4 in toluene.

The intensities of the resonance lines do not directly reflect the radical concentrations. They are altered by electron spin polarization, primarily stemming from triplet polarization. The rise of the magnetization after the formation of the radicals and the simultaneous relaxation of the polarization and the chemical decay of these unstable species can be nicely followed for both radicals. In contrast to TR-ESR, the phosphinoyl radical is difficult to detect by standard ESR due to its short lifetime and the resulting low average concentration.

The initiation step of an acrylate polymerization can be studied using methyl 2-*tert*-butylacrylate 9 as a “non-polymerizing” model for an acrylate. While the addition of the initiating radical to the 3-position of the monomer can easily occur, further reactions of the resulting radical are rendered difficult by the steric bulk of the *tert*-butyl group. Hydrogen abstraction, but no polymerization, is thus observed for these radicals.

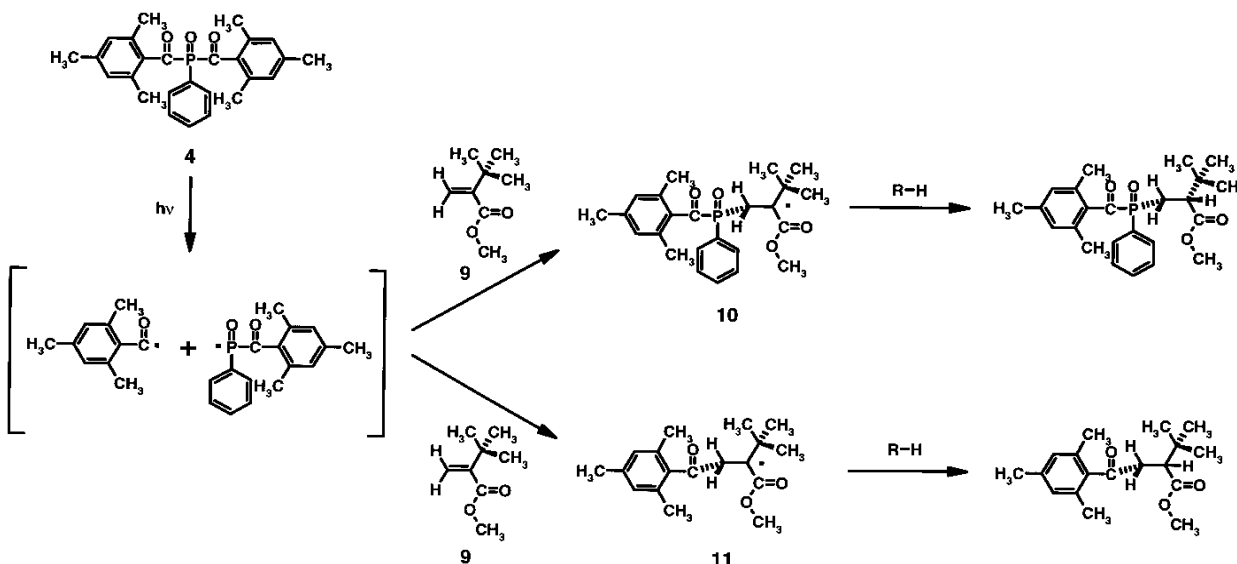


Figure 7. Irradiation of bisacylphosphine oxide 4 in the presence of methyl 2-*tert*-butylacrylate 9.

The following ESR and TR-ESR spectra, which were obtained from BAPO **4** as a photoinitiator and compound **9** (Figure 7), give an instructive insight into the differences of these two closely related techniques.

An ESR spectrum recorded with a flow system during irradiation of the new BAPO photoinitiator **4** in the presence of an excess of methyl 2-*tert*-butylacrylate **9** in toluene is shown in Figure 8. The most prominent signals are those of product **10**, obtained upon addition of the phosphinoyl radical to the acrylate double bond. The large hyperfine coupling of 7.14 mT is due to the interaction of the electron spin with the phosphorus nucleus, while the smaller coupling of 1.30 mT, resulting in a triplet structure and an alternating linewidth effect, is attributed to the coupling with the methylene group. The degeneracy of the coupling constants of the two protons is accidental.

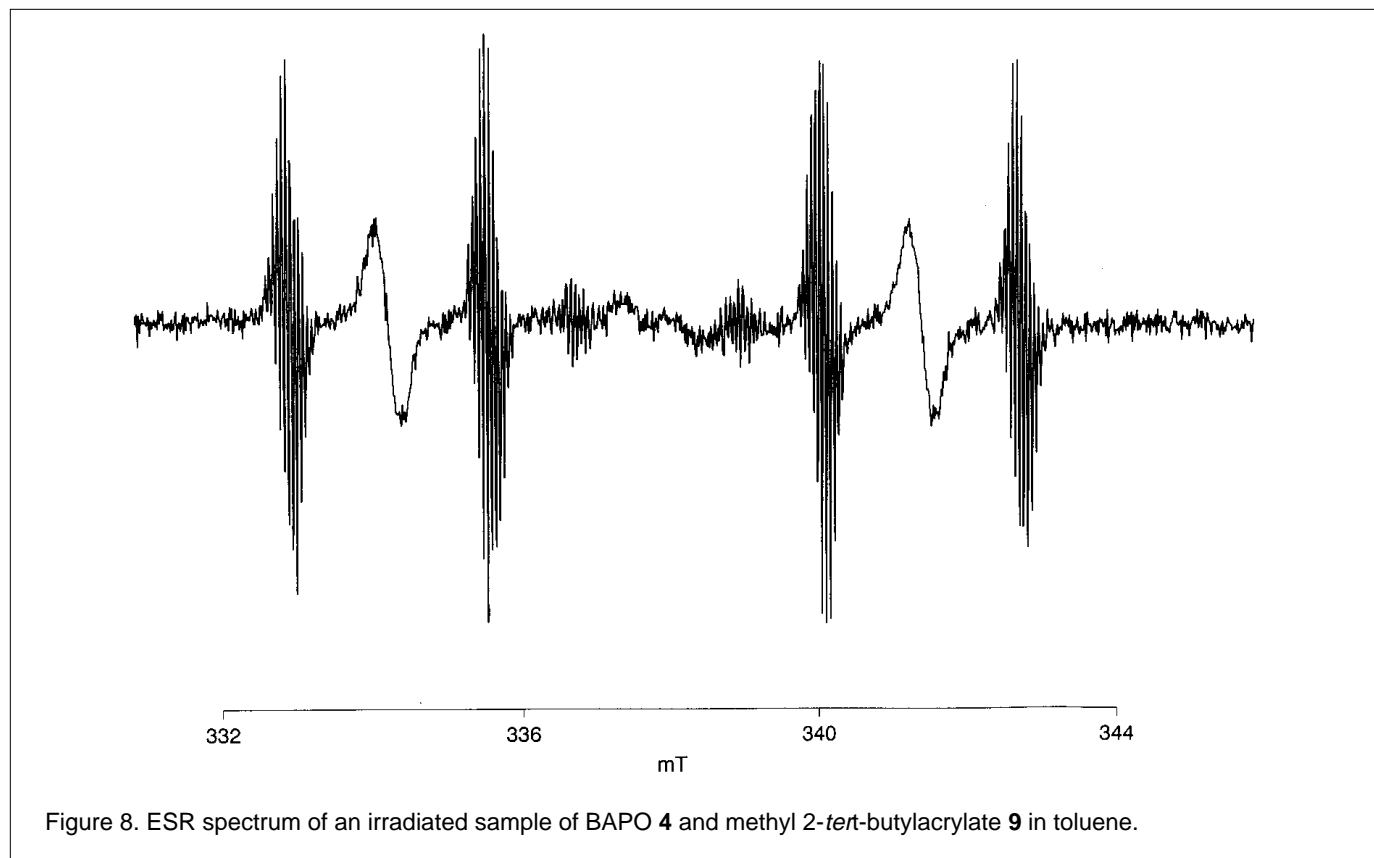


Figure 8. ESR spectrum of an irradiated sample of BAPO **4** and methyl 2-*tert*-butylacrylate **9** in toluene.

The addition product of the benzoyl radical to the model acrylate (radical **11**) is barely visible in the center of the spectrum shown in Figure 8. It consists of a doublet of doublets due to coupling with the methylene protons, with the sum of the two coupling constants being approximately 2.2 mT. The hindered rotation of the methylene protons again leads to a broadening of the two center lines. The small coupling of about 0.07 mT observed in the resonance signals of both compounds is assigned to the protons of the *tert*-butyl group.

Assuming that the life time of these relatively stable adducts does not affect the spectral intensities when a flow system is used, the ratio of the ESR-intensities directly reflects the ratio of the addition constants. The signals of the two addition products in Figure 8 are clear evidence that the addition of phosphorous radicals to an acrylate double bond is more efficient by at least one order of magnitude than that of the benzoyl radical.

The addition of the primary radicals formed from BAPO **4** to the model acrylate **9** was subsequently studied by TR-ESR experiments. In Figure 9 the TR-ESR intensities integrated over different time intervals after the laser pulse are reproduced.

Up to 100 nsec, only the two primary radicals are visible. In the interval between 300 and 400 nsec, the resonance for the phosphinoyl adduct **10** appears. Compared with the first spectrum, the linewidth of the resonances assigned to the primary radicals has decreased. Lifetime broadening effects during the build-up of magnetization by the microwave field (approximately during the first 100 nsec) can no longer be observed. Between 700 and 900 nsec, the phosphinoyl adduct **10** has become dominant. A small benzoyl absorption is still present, while the signals of the phosphinoyl radical are no longer detected. These changes are again proof for the much higher reactivity of the

phosphinoyl radical. Both ESR and TR-ESR are therefore powerful techniques to compare the relative efficiencies of addition reactions quickly in a semiquantitative way.

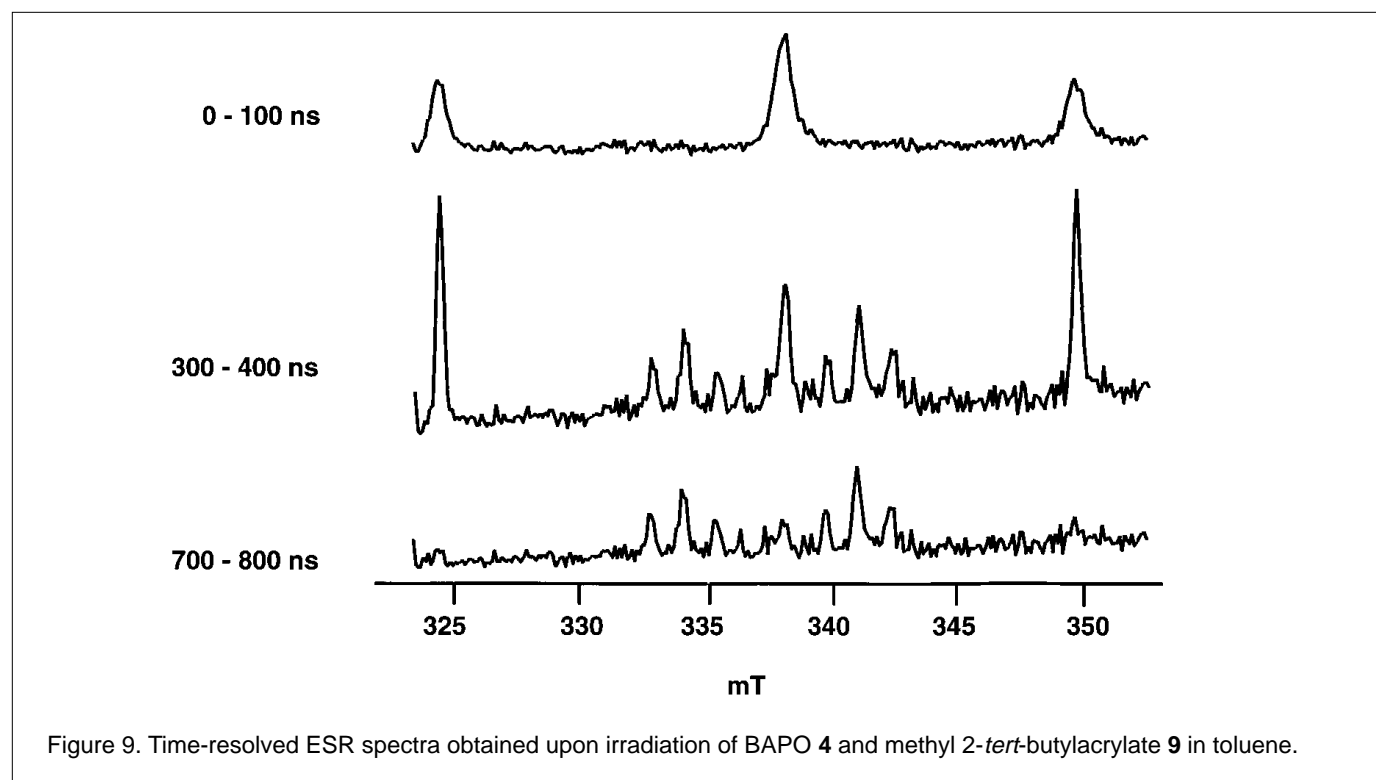
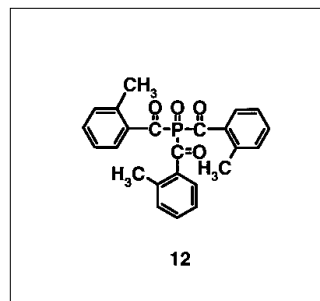


Figure 9. Time-resolved ESR spectra obtained upon irradiation of BAPO **4** and methyl 2-*tert*-butylacrylate **9** in toluene.

Recently the search for more efficient photoinitiators led to the synthesis of a series of trisacylphosphine oxides (TAPO) such as compound **12**.



CIDNP experiments with a nitroxyl trapping agent (TEMPO), analogous to those performed with BAPO compounds, gave evidence that TAPO photoinitiators can undergo three stepwise α -cleavage reactions. This results in the overall formation of six radicals from one photoinitiator molecule.

Some of the new TAPO photoinitiators were investigated by TR-ESR spectroscopy. The TR-ESR spectrum (toluene solution) of compound **12** is reproduced in Figure 10.

Interestingly, triplet polarization is no longer the main enhancement mechanism in this TR-ESR-experiment. This is in contrast to the results obtained in similar experiments using a MAPO photoinitiator (2,4,6-trimethylbenzoyl-diphenylphosphine oxide) or BAPO **4**, where the triplet mechanism is responsible for the dominant polarization. The spectrum of the phosphinoyl radical obtained from **12** exhibits a strong component of radical pair polarization. This is manifested by the emission character of the resonance at low field and the enhanced absorption of the high field transition of the phosphorus centered radical. This polarization effect is typically observed at high radical concentrations when a large number of radical encounter pairs are formed. Taking into account that the molar extinction coefficient of the BAPO **4** at 355 nm is about twice that of TAPO **12**, this finding is good evidence for a higher efficiency of α -cleavage (quantum yield) of TAPO compounds.

The phosphinoyl radical is characterized by a hyperfine coupling of 22.2 mT and a g -value of 2.0038. This hyperfine coupling is significantly smaller than that measured for phosphinoyl radicals generated from the MAPO compound 2,4,6-trimethylbenzoyl-diphenylphosphine oxide (36.5 mT), or that of the corresponding radicals from BAPO **4** (27.2 mT). This decrease of the hyperfine coupling constant is at least partly related to a change in conformation of the phosphinoyl radicals from a pyramidal to a more planar structure.^{17,19}

The conformational changes towards more planar structures leads to increasing p -character and possibly to spin delocalization in the phosphinoyl radical. Due to these changes, the more planar radicals are expected to be less

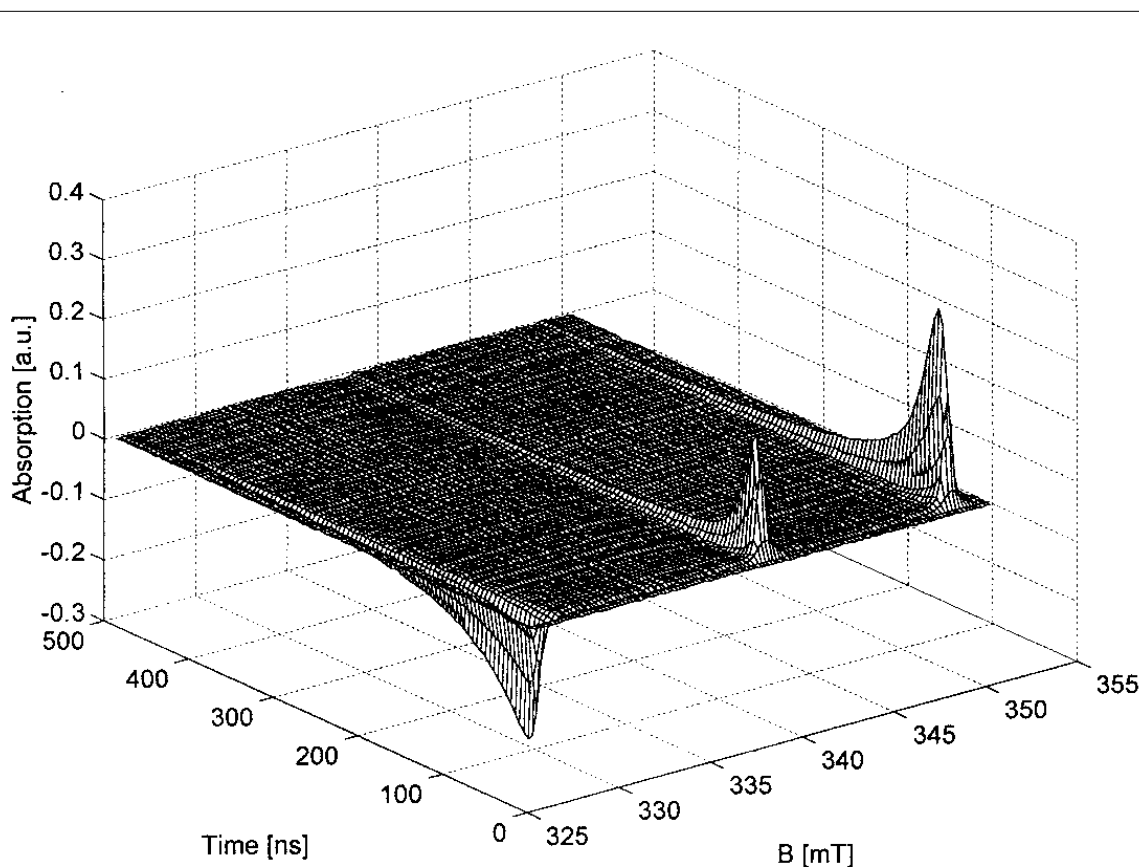


Figure 10. Time-resolved ESR spectra obtained during irradiation of TAPO 12 in toluene.

reactive in addition reactions. In fact, in the same series of photoinitiators, the addition constant of the phosphinoyl radical to methyl methacrylate in toluene solution drops from $4.0 \times 10^7 \text{ Mol}^{-1} \text{ s}^{-1}$ for the MAPO compound to $1.0 \times 10^7 \text{ Mol}^{-1} \text{ s}^{-1}$ for the TAPO initiator.²⁰ Provided that electronic effects are dominant, the hyperfine coupling constant, which can be easily measured, provides an indication of the relative reactivity of phosphinoyl radicals.

However, the overall initiation performance of a photoinitiator is not only controlled by the reactivity of the radicals formed. The smaller addition constant of the phosphinoyl radicals obtained from BAPO or TAPO compounds is more than compensated by their higher absorption and by their ability to form four, respectively six initiating radicals as shown by CIDNP-experiments.

Conclusions

Time resolved ESR and CIDNP spectroscopy are two versatile tools for the investigation of photoinitiators. The two techniques are complementary: ESR allows the direct observation of radical species, while CIDNP-NMR leads to a general view of products derived from radical precursors. Thus the formation of the initiating radicals, the initiation of polymerization and the formation of by-products can easily be studied. An advantage of both techniques, compared to other methods, is the detailed structural information which can be derived from the spectra. Even conformational changes in a series of differently substituted radical intermediates can be detected and related to the chemical reactivity of the species involved. If polarization effects can be estimated or excluded, the two methods also allow for a quantitative analysis of the photochemical reactions.

A limitation of these methods is the lower sensitivity and time resolution compared to techniques based on optical methods, such as laser flash spectroscopy.

Acknowledgment

The authors would like to thank Prof. J. Wirz, University of Basel, for his continuous support and the use of his equipment to perform optical measurements.

References

1. *Chemistry and Technology of UV and EB Formulation for Coatings, Inks and Paints*; Oldring, P.K.T., Ed.; SITA Technology Ltd.: London, 1991; Vol. 1-4.
2. *Radiation Curing in Polymer Science and Technology*; Fouassier, J.P.; Rabek, J.F., Eds.; Elsevier Applied Science: London and New York, 1993; Vol. I - IV.
3. Kirchmayr, R.; Berner, G.; Hüsler, R.; Rist, G. *Farbe + Lack* **1982**, *88*, 910.
4. Jaegermann, P.; Lenzian, F.; Rist, G.; Möbius, K. *Chem. Phys. Lett.* **1987**, *140*, 615.
5. Rist, G.; Borer, A.; Dietliker, K.; Desobry, V.; Fouassier, J. P.; Ruhlmann, D. *Macromolecules* **1992**, *25*, 4182.
6. Kolczak, U.; Rist, G.; Dietliker, K.; Wirz, J. *J. Am. Chem. Soc.* **1996**, *118*, 6477.
7. McLauchlan, K.A.; Yeung, M.T. In *Specialised Periodical Reports, Electron Spin Resonance*; The Royal Society of Chemistry: Cambridge, 1994; Vol. 14, p 32.
8. Forbes, M.D.E. *The Spectrum* **1995**, *8*, 1.
9. Adrian, G.J. *J. Chem. Soc. Chem. Comm.* **1971**, 732.
10. Kaptein, R.J. *Am. Chem. Soc.* **1972**, *94*, 6251.
11. Jacobi, M.; Henne, A.J. *Rad. Curing* **1983**, *19(4)*, 16.
12. Jacobi, M.; Henne, A.; Boettcher, A. *Polym. Paint. Colour J.* **1985**, *175*, 636.
13. Leppard, D.; Dietliker, K.; Hug, G.; Kaeser, R.; Köhler, M.; Kolczak, U.; Misev, L.; Rist, G.; Rutsch, W.; *Proc. Radtech '94 North America*; Vol. II; 1994; p 693.
14. Rutsch, W.; Dietliker, K.; Leppard, D.; Köhler, M.; Misev, L.; Kolczak, U.; Rist, G. *Prog. Org. Coatings* **1996**, *27*, 227.
15. Leppard, D.G.; Köhler, M.; Hug, G. PCT Patent Appl. WO 96/07662 (Prior. 8.9.94) to Ciba Specialty Chemicals Inc.
16. Baxter, J.E.; Davidson, R.S.; Hageman, H.J.; McLauchlan, K.A.; Stevens, D.G. *Chem. Soc., Chem. Commun.* **1987**, 73.
17. Slugett, G.W.; McGarry, P.F.; Koptuyg, I.V.; Turro, N.J. *J. Am. Chem. Soc.* **1996**, *118*, 7367.
18. Dietliker, K.; Leppard, D.; Jung, T.; Köhler, M.; Valet, A.; Kolczak, U.; Rzedek, P.; Rist, G. *Conf. Proceedings RadTech Asia 97*; Yokohama: 1997, p 292.
19. Sumiyoshi, T.; Schnabel, W. *Makromol. Chem.* **1985**, *186*, 1811.
20. Rzedek, P.; Rist, G.; Wirz, J.; unpublished results.

About the Authors

Kurt Dietliker and David Leppard are research chemists at the Research Center Marly of Ciba Specialty Chemicals. In collaboration with Martin Kunz of the Application Laboratories in Basel, they are responsible for the development of new photoinitiators for the Additives Division of Ciba Specialty Chemicals Inc. Dr. Dietliker's address is Ciba SC Recherche Marly SA, Research Center Marly, P.O. Box 64, CH-1723 Marly, Switzerland.

Günther Rist is responsible for the ESR and CIDNP laboratories of Novartis Services AG in Basel. Together with Urszula Kolczak (current address: University of California, Davis, USA) and the doctoral students Iwo Gatlik and Piotr Rzedek, he investigates the photochemistry of new photoinitiators using these techniques.

The Spectrum on the World-Wide Web

The Spectrum is available on the Center's Web site: <http://www.bgsu.edu/departments/photochem/>. You can access via Acrobat Reader. There are instructions for downloading a free copy of Acrobat Reader from the Adobe Web site.

If you plan to access *The Spectrum* electronically, please send an e-mail to: photochemical@listproc.bgsu.edu. We will remove you from our paper mailing list. Please browse our Web site for up-to-date information about the Center and its programs.

Center for Photochemical Sciences Publications

291. Grinevich, O.; **Snively, D.L.** Vibrational overtone enhancement of methyl methacrylate polymerization initiated by benzoyl peroxide decomposition, *Chem. Phys. Lett.* **1997**, 267, 313.
292. Arudchandran, A.; **Bullerjahn, G.S.** Expression of the *petE* gene encoding plastocyanin in the photosynthetic prokaryote, *Prochlorothrix hollandica*, *Biochem. Biophys. Res. Comm.* **1996**, 226, 220.
293. Morlino, E.A.; **Rodgers, M.A.J.** Nitric oxide deligation from nitrosyl complexes of two transition metal porphyrins: a photokinetic investigation, *J. Am. Chem. Soc.* **1996**, 118, 11798-11804.
294. Aloisi, G.G.; Elisei, F.; Latterini, L.; Mazzucato, U.; **Rodgers, M.A.J.** Excited state behavior of diarylethenes in the subnanosecond time-scale; the role of an upper singlet, *J. Am. Chem. Soc.* **1996**, 118, 10879-10887.
- * 295. Logunov, S.L.; **Rodgers, M.A.J.** Charge recombination reactions in self-assembled porphyrin-based ion-pair complexes, *J. Photochem. Photobio., A*, in press.
- * 296. **Midden, W.R.** Rounding numbers: why the new system doesn't work, *J. Chem. Ed.*, in press.
297. Hu, S.; **Neckers, D.C.** Lifetime of the 1,4-biradical derived from alkyl phenylglyoxylate triplets: an estimation using the cyclopropylmethyl radical clock, *J. Org. Chem.* **1996**, 62(3), 755-757.
- * 298. Mejiritski, A.; Polykarpov, A.Y.; Sarker, A.M.; **Neckers, D.C.** Quantum yield determination for photolysis of photoimageable polymer in thin films, *J. Photochem. Photobio., A: Chem.*, in press.
299. Fedorov, A.; **Snively, D.L.** Vibrational overtone spectroscopy of butadiene iron tricarbonyl and 1,3-butadiene, *J. Phys. Chem. A*, **1997**, 101, 1451.
300. Jager, W.F.; Lungu, A.; Chen, D.Y.; **Neckers, D.C.** Photopolymerization of polyfunctional acrylates and methacrylate mixtures. Characterization of polymeric networks by a combination of fluorescence spectroscopy and solid state NMR, *Macromolecules* **1997**, 30, 780.
301. Hu, Shengkui; **Neckers, D.C.** Photochemical reactions of mercapto/amino substituted alkyl phenylglyoxylates induced by intramolecular electron abstraction, *Tetrahedron* **1997**, 58(8), 2751-2766.
- * 302. Lungu, A.; **Neckers, D.C.** Structural conformations of some photopolymerized dimethacrylates by solid-state NMR. A $C^{13} T_{1\rho}$ relaxation times study, submitted for publication in *J. Polym. Sci.*
- * 303. Mejiritski, A.; Sarker, A.M.; Wheaton, B.; **Neckers, D.C.** Novel method of thermal epoxy curing based on photogeneration of polymeric amines and negative-tone image formation, *Chem. Mat.*, **1997**, in press.
304. Ford, W.E.; **Rodgers, M.A.J.** Kinetics of nitroxyl oxidation by Ru(bpy)₃³⁺ following photosensitization of antimony-doped tin dioxide colloidal particles, *J. Phys. Chem.* **1997**, 101, 930-936.
305. Gorman, A.A.; Hamblett, I.; Hill, T.J.; Jones, H.; **Srinivasan, V.S.** Wood, P.D. Curcumin: A pulse radiolysis investigation of the radical in micellar systems, *ACS Symposium Series 600* **1997**, 234-243.

For reprints of any of these publications, please write the Center for Photochemical Sciences and refer to the reprint by number. Reprints of articles in press will be provided upon publication of the article.

- * As soon as an article is accepted for publication, the Center assigns a number and lists them accordingly for internal recordkeeping.

Celebration of the "Photochemical Tie to 1938"

In appreciation of the contributions of six photochemists born in the year of 1938, a symposium will be held. The symposium will take place during the Fall 1998 ACS National Meeting (August 23-27, 1998) in Boston. You are cordially invited to participate in this historical event.

Honorees (will also speak at the symposium):

R. S. H. Liu	N. J. Turro
D. C. Neckers	P. Wagner
J. Saltiel	D. G. Whitten

Speakers at the symposium include the following:

P. F. Barbara	T. Gilbro	I. Kochevar	G. B. Schuster
J. Barton	R. S. Givens	C. V. Kumar	R. Schwerzel
I. Bronstein	J. Goodman	F. D. Lewis	Y. Shicbida
R. Caldwell	I. Gould	J. Michl	S. C. Shim
W. J. DeGrip	H. B. Gray	K. Nakanishi	M. Sponsler
F. Deschryver	G. S. Hammond	D. Nocera	J. K. Thomas
K. Deshayes	E. Hilinski	M. B. Platz	L. Tolbert
M. El Sayed	H. Inoue	M. A. J. Rodgers	M. Tsuda
S. Farid	Y. Inoue	J. C. Scaiano	C. Turro
M. Forbes	M. Irie	K. Schanze	D. Waldek
M. A. Fox	W. F. Jager	J. R. Scheffer	R. G. Weiss
E. Gaillard	W. J. Jenks	R. Schmehl	O. C. Zafiriou
M. Garcia-Garibay	M. Kasha	D. I. Schuster	R. G. Zepp
			M. B. Zimmt

For details, see the world wide web site at <http://www.chem.fsu.edu/photo38.htm> or check the IAPS homepage for a hotlink. For information on the symposium contact:

V. Ramamurthy
 Department of Chemistry
 Tulane University
 New Orleans, LA 70118
 Tel: (504) 862-8135
 Fax: (504) 865-5596
 E-mail: murthy@mailhost.tcs.tulane.edu

Russell H. Schmehl
 Department of Chemistry
 Tulane University
 New Orleans, LA 70118
 Tel: (504) 865-5573
 Fax: (504) 865-5596
 E-mail: schmehl@mailhost.tcs.tulane.edu

Kurt D. Deshayes
 Department of Chemistry
 Bowling Green State University
 Bowling Green, OH 43403
 Tel: (419) 372-2470
 E-mail: kdeshay@opie.bgsu.edu

Matthew B. Zimmt
 Department of Chemistry
 Brown University
 Providence, RI 02912
 Tel: (401) 863-2909
 E-mail: Matthew_Zimmt@brown.edu

A special issue of the *Journal of Physical Chemistry* will be published preceding the symposium. If you are interested in publishing an article in this special issue as per the guidelines of the journal, please contact one of the following:

V. Ramamurthy (murthy@mailhost.tcs.tulane.edu)
 M. Garcia Garibay (mgg@chem.ucla.edu)
 R. H. Schmehl (schmehl@mailhost.tcs.tulane.edu)